Title page

Unmasking Hidden Systemic Effects of Neurodegenerative Diseases: A Two-Pronged Approach to Biomarker Discovery

Sandra I. Anjo[1,2,3,4,*,†], Miguel Rosado[1,2,3,5,*], Inês Baldeiras[1,2,6], Andreia Gomes[7], Diana Pires[7], Cátia Santa[1,2,3], Joana Pinto[1,2], Cristina Januário[6], Isabel Santana[1,2,6], Ana Verdelho[8,9], Alexandre de Mendonça[9], Miguel Castelo-Branco[7,#], Bruno Manadas[1,2,3#,†]

[1] CNC - Centro de Neurociências e Biologia Celular, Universidade de Coimbra, Rua Larga - Faculdade de Medicina, 1ºandar - POLO I, 3004-504 Coimbra, Portugal.

[2] CIBB - Centre for Innovative Biomedicine and Biotechnology, University of Coimbra, Rua Larga - Faculdade de Medicina, 1ºandar - POLO I, 3004-504 Coimbra, Portugal.

[3] Instituto de Investigação Interdisciplinar, Universidade de Coimbra (IIIUC), Casa Costa Alemão, R. Dom Francisco de Lemos, 3030-789 Coimbra, Portugal.

[4] Faculdade de Medicina, Universidade de Coimbra, Azinhaga de Santa Comba, 3000-548 Coimbra, Portugal.

[5] - University of Coimbra, Institute for Interdisciplinary Research, Doctoral Programme in Experimental Biology and Biomedicine (PDBEB), Portugal

[6] Serviço de Neurologia, Centro Hospitalar e Universitário de Coimbra, Praceta Professor Mota Pinto, 3004-561 Coimbra, Portugal.

[7] Coimbra Institute for Biomedical Imaging and Translational Research (CIBIT), Azinhaga de. Santa Comba, 3000-548 Coimbra, Portugal.

[8] Department of Neurosciences and Mental Health, Santa Maria Hospital - CHLN, ISAMB, University of Lisbon, Av. Prof. Egas Moniz MB, 1649-028 Lisboa, Portugal.

23 [9] Instituto de Medicina Molecular e Faculdade de Medicina, Universidade de Lisboa, Av. Prof. Egas
24 Moniz, 1649-028 Lisboa, Portugal.

25 * - Equal contribution

26 # - Senior equal contribution

27 † - Corresponding authors: Bruno Manadas (bmanadas@cnc.uc.pt, +351231249170) and Sandra Anjo
28 (sandra.anjo@cnc.uc.pt, +351231249170), Center for Neuroscience and Cell Biology – University of
29 Coimbra, UC Biotech - Parque Tecnológico de Cantanhede, Núcleo 04, Lote 8, 3060-197 Cantanhede –
30 Portugal

31 E-mail addresses: Miguel Rosado - mmva.rosado@gmail.com; Ines Baldeiras - ibaldeiras@cnc.uc.pt;
32 Andreia Gomes - andmaggomes@gmail.com; Diana Pires - diana.santos.pires@gmail.com; Cátia Santa -
33 catiajmsanta@gmail.com; Joana Pinto - joana.amaralpinto@gmail.com; Cristina Januário -
34 cristinajanuario@gmail.com; Isabel Santana - isabeljsantana@gmail.com; Ana Verdelho -
35 averdelho@medicina.ulisboa.pt; Alexandre de Mendonça - mendonca@medicina.ulisboa.pt; Miguel
36 Castelo-Branco - mcbranco@fmed.uc.pt.

37 **Running head and abbreviations**

38 Dual Approach to Serum Biomarker Discovery

39 AD, Alzheimer's Disease; APOA1-HDL, High-Density Lipoproteins containing Apolipoprotein A1; AUC,
40 Area Under the Curve; Aβ, Amyloid-β; BBB, Blood-Brain Barrier; BioGRID, Biological General Repository
41 for Interaction Datasets; CE, Collision Energy; CES, Collision Energy Spread; CHUC, Centro Hospitalar e
42 Universitário de Coimbra; CI, Confidence Interval; CNS, Central Nervous System; CT, Healthy Controls;
43 DDA, Data-dependent Acquisition; DMSO, Dimethyl Sulfoxide; FA Formic Acid; FDR, False Discovery
44 Rate; GO, Gene Ontology; HDL, High-Density Lipoproteins; HMW, High Molecular Weight; IS, Internal
45 Standard; LDA, Linear Discriminant Analysis; MCI, Mild Cognitive Impairment; MS, Mass Spectrometry;
46 MW, Molecular Weight; MWCO, Molecular Weight Cut-Off; NDs, Neurodegenerative Diseases; PD,
47 Parkinson's Disease; ROC, Receiver Operating Curve; SE, Standard Error; STRING, Search Tool for
48 Retrieval of Interacting Genes/Proteins; XIC, Extracted Ion Chromatogram.

Abstract

Identification of reliable blood biomarkers for neurodegenerative diseases (NDs) is crucial for translational and clinical research. However, conventional omics struggle with blood samples complexity, hindering desired outcomes. In this work the potential of High Molecular Weight (HMW) fractionation under non-denaturing conditions as a complementary approach to the conventional proteomics for identifying serum biomarkers in NDs was explored. A cohort of 58 serum samples of Alzheimer's disease (AD), Parkinson's disease (PD) patients and control (CT) individuals was used to compare the two proteomics strategies: i) direct analysis of whole serum and ii) non-denaturing fractionation using 300 kDa cut-off filters (HMW serum).

Although both approaches quantified a similar set of proteins, each approach captured a distinct subset of differentially altered proteins, suggesting that HMW fractionation identified additional types of alterations beyond conventional protein level changes. A discriminant model combining altered proteins from both datasets effectively distinguished between the three groups (AUC = 0.999 and median sensitivity and specificity of 97.4% and 91.7%, respectively). Importantly, this performance surpassed that of any model created using each method individually.

Altogether, this work demonstrated that HMW fractionation can be a valuable complementary method to direct serum analysis and could enhance biomarker discovery. The 10 proteins included in the model (5 from each strategy), comprise clear evidence for the contribution of apolipoproteins for the diagnosis of NDs, revealing potential changes within lipid metabolism and the organization of macromolecules and their complexes, thereby uncovering effects that remain hidden from a conventional serum proteome analysis.

71 **Keywords**

72 Serum Proteomics

73 High Molecular Weight Fractionation

74 Neurodegenerative Diseases

75 SWATH-MS/DIA

76 Protein complexes/Proteoforms

77 Apolipoproteins

78 Lipoproteins

79

Introduction

Proteins can be directly or indirectly related to a myriad of diseases, thereby being important targets of biomarker research, which remains a pivotal aspect of clinical research. However, biomarker discovery based on conventional proteomics strategies has not yet yielded substantial practical applications. Blood and its fractions are the most studied samples for biomarker identification, not only due to easy accessibility but also because of its interactions with most tissues in the body, potentially reflecting disease-related alterations [1, 2]. However, both plasma and serum proteomes have a large dynamic range of protein concentrations [1], with the detection of those least abundant being masked by the most abundant. Despite all the technical developments in proteomics quantification by mass spectrometry (MS) [3], the high dynamic range still precludes the complete characterization of these samples, which may be one of the reasons why the identification of relevant biomarkers in plasma/serum by MS remains challenging [4]. Therefore, it is essential to have alternative approaches to the direct analysis of these highly demanding biofluids. Several approaches have been developed to reduce sample complexity [5], such as size exclusion chromatography and electrophoretic separation methods. When dealing with numerous samples, a more straightforward approach that could serve as an alternative to direct sample analysis is centrifugal ultrafiltration [5]. This approach relies on the separation of sample components based on size exclusion, which is correlated to molecular weight (MW). This method has typically been used to study the low molecular weight proteome of serum and plasma samples, using filters between 20 kDa and 40 kDa [6, 7], but it may also be used to study other proteome fractions. Alzheimer's Disease (AD) and Parkinson's Disease (PD) are inherently linked to protein aggregation [8] and, therefore, to the formation of high molecular weight (HMW) protein complexes. Fractionation of peripheral fluid samples from patients with these diseases, focused on the HMW proteome, could be useful to eliminate high abundance proteins and to study protein aggregates that may be present in circulation. In this study, we propose using centrifugal ultrafiltration focused on the HMW proteome, not as an alternative but as a complementary analysis to the investigation of unfractionated samples, to potentially assess the restructuring of molecular complexes as a distinctive feature of disease. To evaluate our hypothesis, the same set of samples was subjected to the proteomics analysis of the whole serum and fractionation using centrifugal ultrafiltration with 300 kDa

108 molecular weight cut-off (MWCO) filters in a non-denaturing environment (henceforth referred to as
109 HMW fractionation). The data obtained from both approaches were directly compared and merged to
110 identify potential biomarkers. This study used a cohort consisting of patients with neurodegenerative
111 disorders, specifically Alzheimer's and Parkinson's disease patients, and healthy controls (CT) to test the
112 significance of using HMW fractionation as a complementary tool for biomarker discovery. These
113 disorders were chosen as they are considered as potential proteinopathies, making them promising
114 targets for this research.

115

116 ## Materials and Methods

117 ### Participants

118 A total of 58 serum samples were used in this study, comprising 3 groups of individuals: AD (n = 22), PD
119 (n = 24), and CT (n = 12). The PD patients were recruited at the Movement Disorders Units of the
120 Neurological Department of the CHUC, where they were assessed by a movement disorders specialist
121 and were diagnosed according to the criteria defined by the UK Parkinsons's Disease Society Brain Bank
122 [9]. The exclusion criteria for these patients consisted of severe dementia (as indicated by a Mini-Mental
123 State Exam score below 15), any psychiatric disorder, or other forms of Parkinsonism. The clinical group
124 of individuals with AD diagnosis was recruited and prospectively evaluated by two experienced
125 neurologists at Memoclínica and the Neurology Department of the CHUC. The standard criteria for the
126 diagnosis of AD were the Diagnostic and Statistical Manual of Mental Disorders—fourth edition (DSM-
127 IV-TR) [10] and the National Institute on Aging and the Alzheimer's Association Workgroup [11]. To
128 ensure the homogeneity of the sample, only patients who met the following criteria were included: they
129 were in a stable condition, did not sustain recent changes in medication, and did not have
130 ophthalmological or neurological/psychiatric conditions other than AD. The CT group was composed of
131 age- and gender-matched individuals from the community with no history of cognitive deterioration,
132 neurological or acquired central nervous system (CNS) disorders, traumatic brain injury, or psychiatric
133 disorders. The CT group was also submitted to a brief cognitive assessment to exclude the presence of
134 cognitive impairment.

135 ### Serum processing for proteomics analysis

136 Two different strategies were used to obtain a more comprehensive proteomic characterization of
137 serum samples, namely: i) direct analysis of whole serum and ii) HMW fractionation through
138 ultrafiltration using 300 kDa cut-off filters (HMW serum).

139 For each sample, 5 µL were used for direct serum analysis and 82.5 µL for HMW serum fractionation.
140 Additionally, three sample pools were prepared by combining aliquots of all the samples, for the AD
141 pool, PD pool, and CT pool, respectively. Pooled samples were used for Data-dependent acquisition

142 (DDA) experiments to build a specific protein library to be used in data-independent acquisition (DIA)
143 analysis and were subjected to the same sample processing as the individual samples. Before
144 processing, all samples were spiked with the same amount of an internal standard (IS) to account for
145 sample loss [12]. Different internal standards were used depending on the type of analysis: MBP-GFP
146 [12] in the case of the whole serum approach, while equine ferritin, commonly available as one of the
147 standards in the Gel Filtration Calibrants Kit for High Molecular Weight proteins (GE28-4038-42), for the
148 HMW fractionation approach.

149 For the direct analysis of whole serum, the samples were diluted in Laemmli buffer, followed by
150 denaturation for 5 min at 95°C and cysteine alkylation with acrylamide, and the total volume in all
151 samples was subjected to in-gel digestion using the Short-GeLC for subsequent quantitative analysis by
152 LC-MS/MS-DIA [13].

153 Samples subjected to HMW fractionation were ultrafiltrated using 300 kDa cut-off filters (Vivaspin® 500
154 Polyethersulfone, 300 kDa (Sartorius)) pre-conditioned to PBS. Serum samples were diluted into 200 µL
155 of PBS and subjected to 20 min centrifugation at 14,500× g at 4 °C followed by an additional washing
156 step with another 200 µL of PBS. In some cases, the washing step was repeated until the retentate
157 volume did not exceed 50 µL. The resulting retentates, the HMW fraction, were collected into a new
158 LoBind® microcentrifuge tube and precipitated with ice-cold acetone [14]. The precipitated pellets were
159 resuspended into 30 µL of a solution containing 2% SDS (v/v) and 1 M of Urea, always aided by
160 sonication (VibraCell 750 watt-Sonics ®) with ice in the cup horn (2 min. pulse duration, at 1 second
161 intervals, and with 40% amplitude). Afterward, concentrated Laemmli Buffer was added to the samples,
162 followed by a 30 min incubation to reduce the samples and a 20 min incubation with iodoacetamide for
163 cysteine alkylation [15]. The total volume in all samples was subjected to in-gel digestion as previously
164 specified [13].

165 **Mass spectrometry data acquisition**

166 Samples were analyzed on a NanoLC™ 425 System (Eksigent®) couple to a TripleTOF™ 6600 System
167 (Sciex®) using DDA for each fraction of the pooled samples for protein identification and SWATH-MS
168 acquisition of each sample for protein quantification. Peptides were resolved by micro-flow liquid

169 chromatography on a MicroLC column ChromXP™ C18CL (300 µm ID × 15 cm length, 3 µm particles, 120
170 Å pore size, Eksigent®) at 5 µL/min. The liquid chromatography program was performed as follows with
171 a multistep gradient: 2 % to 5 % mobile phase B (0-2 min), 5 % to 28 % B (2-50 min), 28% to 35% B (50-
172 51 min), 35 to 98% of B (50–52 min), 98% of B (52-61 min), 98 to 2% of B (61–62 min), 2% of B (68 min).
173 Mobile phase A was composed of 0.1 % formic acid (FA) with 5% dimethyl sulfoxide (DMSO), and mobile
174 phase B was composed of 0.1 % FA and 5% DMSO in acetonitrile. Peptides were eluted into the mass
175 spectrometer using an electrospray ionization source (DuoSpray™ Source, ABSciex®) with a 25 µm
176 internal diameter hybrid PEEKsil/stainless steel emitter (ABSciex®). The ionization source was operated
177 in the positive mode set to an ion spray voltage of 5 500 V, 25 psi for nebulizer gas 1 (GS1) and 25 psi for
178 the curtain gas (CUR).

179 For DDA experiments, the mass spectrometer was set to scan full spectra (m/z 350-1250) for 250 ms,
180 followed by up to 100 MS/MS scans (m/z 100–1500) per cycle to maintain a cycle time of 3.309 s. The
181 accumulation time of each MS/MS scan was adjusted in accordance with the precursor intensity
182 (minimum of 30 ms for precursor above the intensity threshold of 1000). Candidate ions with a charge
183 state between +2 and +5 and counts above a minimum threshold of 10 counts per second were isolated
184 for fragmentation and one MS/MS spectrum was collected before adding those ions to the exclusion list
185 for 25 seconds (mass spectrometer was operated by Analyst® TF 1.7, ABSciex®). The rolling collision
186 energy (CE) was used with a collision energy spread (CES) of 5.

187 For SWATH-MS-based experiments, the mass spectrometer was operated in a looped product ion mode
188 [16] and the same chromatographic conditions were used as in the DDA experiments described above. A
189 set of 60 windows of variable width (containing 1 m/z for the window overlap) was constructed,
190 covering the precursor mass range of m/z 350-1250. A 250 ms survey scan (m/z 350-1500 m/z) was
191 acquired at the beginning of each cycle for instrument calibration and SWATH-MS/MS spectra were
192 collected from the precursors ranging from *m/z* 350 to 1250 for *m/z* 100–1500 for 20 ms resulting in a
193 cycle time of 3.304 s. The CE for each window was determined according to the calculation for a charge
194 +2 ion centered upon the window with variable CES according to the window.

195 **Mass spectrometry data processing**

196 A specific library of precursor masses and fragment ions was created by combining all files from the DDA
197 experiments and used for subsequent SWATH processing. Libraries were obtained using ProteinPilot™
198 software (v5.1, ABSciex®), using the following parameters: i) search against a database from SwissProt
199 composed by Homo Sapiens (released in March 2019), and MBP-GFP [15] and horse ferritin light and
200 heavy chains sequences ii) acrylamide or iodoacetamide alkylated cysteines, for whole serum or HMW
201 respectively, as fixed modification; iii) trypsin as digestion enzyme and iv) urea denaturation as a special
202 factor in the case of the HMW samples. An independent False Discovery Rate (FDR) analysis using the
203 target-decoy approach provided with Protein Pilot software was used to assess the quality of the
204 identifications, and positive identifications were considered when identified proteins and peptides
205 reached a 5% local FDR [17, 18].

206 Data processing was performed using the SWATH™ processing plug-in for PeakView™ (v2.0.01, AB
207 Sciex®) [19]. After adjustment of retention time using a combination of IS and endogenous peptides, up
208 to 15 peptides, with up to 5 fragments each, were chosen per protein, and quantitation was attempted
209 for all proteins in the library file identified from ProteinPilot™ searches.

210 Protein levels were estimated based on peptides that met the 1% FDR threshold with at least 3
211 transitions in at least six samples in a group, and the peak areas of the target fragment ions of those
212 peptides were extracted across the experiment using an extracted-ion chromatogram (XIC) window of 5
213 minutes with 100 ppm XIC width. Protein levels were estimated by summing all the transitions from all
214 the peptides for a given protein (an adaptation of [20] and further normalized to the levels of the IS
215 [15]).

216 **Statistical analysis and biological interpretation**

217 Pearson's Chi-squared Test for Count Data was performed in R version 4.2.1, using the chisq.test
218 function available in the native stats package in R to determine if there were significant differences in
219 the gender proportion of the groups within the studied cohort.

220 To assess the variation of the serum proteins (either Whole serum or the HMW fraction of the serum)
221 among the three groups, a Kruskal–Wallis H test was followed by the Dunn's Test for pairwise

222 comparison. Dunn's p-values were corrected using the Benjamini-Hochberg FDR adjustment, and
223 statistical significance was considered for p-values below 0.05.

224 Stepwise Linear Discriminant Analysis (LDA) was performed to select the proteins responsible for the
225 best separation of the groups being studied. LDA was performed using IBM® SPSS® Statistics Version 22
226 (Trial). LDA was attempted considering the proteins only altered at the Whole Serum or HMW Serum,
227 and for the combination of both results. The evaluation of the models obtained from each analysis was
228 performed by comparison of the Receiver operating characteristic (ROC) curves obtained using each
229 model. A comparison of the ROC curves was performed using MedCalc Statistical Software version
230 20.106 (MedCalc Software Ltd;[21]; Trial). The Delong et al. (1988) [22] method was used for the
231 calculation of the Standard Error (SE) of the Area Under the Curve (AUC) and of the difference between
232 two AUCs, and the Confidence Interval (CI) for the AUCs were calculated using the exact Binomial
233 Confidence Intervals which are calculated as the following AUC ± 1.96 SE.

234 Violin plots were used to present the distribution of the individual protein levels among each condition,
235 and Pearson's correlation analysis was performed to evaluate the similarity between the profiles of the
236 proteins highlighted in the study. Violin plots were generated using GraphPad Prism 8.0.1 (Trial) and the
237 Pearson's correlation was performed using Morpheus software [23]. Heatmap and hierarchical
238 clustering analyses were computed using PermutMatrix version 1.9.3 [24, 25] using the Euclidean
239 distance and McQuitty's criteria.

240 Physical protein-protein interactions between the highlighted analytes were predicted by GeneMANIA
241 webserver (Gene Function Prediction using a Multiple Association Network Integration Algorithm; [26,
242 27] together with a gene ontology (GO) analysis of the formed network. In addition to the proteins
243 imported from this study, 28 additional related genes were allowed to create the interaction network
244 using equal weighting by network. An additional GO enrichment analysis considering the term
245 "biological process" was also performed. On the other hand, functional protein association networks
246 were evaluated using the Search Tool for Retrieval of Interacting Genes/Proteins (STRING) version 11.5
247 [28] with a medium confidence of 0.4 [29].

Pathway enrichment analyses were performed using the FunRich software (version 3.1.3) [30], considering two different databases: the FunRich or the Reactome database. In both instances, a statistical analysis employing a hypergeometric test was conducted, using the FunRich human genome database as the background. Enriched pathways were considered for a non-corrected or a Bonferroni-corrected p-value below 0.05 for Funrich or Reactome database, respectively.

254 ## Results

255 ### High molecular weight fractionation as a reproducible method for biomarker discovery

256 To explore the potential of HMW fractionation in peripheral biomarker research, serum samples
257 underwent either ultrafiltration using a 300 kDa MWCO filter followed by protein precipitation of the
258 retentate (referred to as HMW serum), before protein digestion and MS analysis, or were directly
259 analyzed (whole serum) (see Figure 1). In the proposed pipeline, the HMW fractionation was performed
260 under non-denaturing conditions, such that the filter would retain native HMW protein complexes and
261 large molecular structures.

262 As previously reported, employing an appropriate IS is crucial for delineating effective proteome
263 changes among different groups [12]. Given the nature of the fractionation proposed in this study, an
264 ideal IS for this procedure would be a HMW protein that remains retained by the filter and bears no
265 similarity to other human proteins. In this context, equine globular protein Ferritin (~440 kDa size)
266 emerged as a suitable IS for several reasons: it lacks similarity with any other protein from the human
267 proteome (Additional File 1: Supplementary Figure 1a), the peptides monitored in the SWATH-MS
268 analysis are easily distinguishable from the matrix (the human serum proteome; Additional File 1:
269 Supplementary Figure 1b), and it exhibits a coefficient of variation similar to the one obtained by the
270 MBP-GFP used in the unfractionated analysis and previously characterized [12] (Additional File 1:
271 Supplementary Figure 1c). Additionally, the overall reproducibility of the fractionation was also
272 inspected. Similarly, to what was observed for the IS (Additional File 1: Supplementary Figure 1c), the
273 overall coefficient of variation of the proteins quantified using technical replicates (Additional File 1:
274 Supplementary Figure 1d) revealed that this procedure did not induce an appreciable increase in the
275 variability of the quantification when compared with the conventional protocol (unfractionated
276 samples). Moreover, the variation caused by the sample processing steps may be reverted by the
277 normalization of the values to the IS since the coefficient of variation of the IS is similar to the one
278 observed for the majority of the proteins, indicating that the selected IS is a good predictor of the
279 alterations induced by the method.

280 ### High molecular weight fractionation increases the detection of proteomic alterations in NDs

281 As proof of concept, this procedure was applied to serum samples of a cohort comprised of 3 different
282 groups: AD (n = 22), PD (n = 24), and CT (n = 12). No statistically significant differences were found in the
283 gender distribution between the three groups; however, differences were observed concerning age
284 distribution, with PD individuals being slightly younger, on average, than both other groups (Table 1).

285 Patients with neurodegenerative diseases, both AD and PD, were selected for this study. These
286 conditions are frequently associated with the development of abnormal protein complexes and protein
287 aggregation. Hence, they offer a fitting context to evaluate the fractionation approach's effectiveness in
288 exploring potentially altered protein interactions—an aspect frequently neglected in conventional
289 proteomics analyses.

290 **Table 1.** Study population distribution across age and sex.

	AD (n = 22)	PD (n = 24)	CT (n = 12)	p-value				
				CT vs. Diseases	CT vs. AD vs. PD	AD vs. PD	CT vs. PD	CT vs. AD
Male (n)	9	11	3	0.197*	-	0.643*	0.148*	0.262*
Female (n)	13	13	9					
Age (mean ± SD)	68.4 ± 8.2	60.3 ± 10.4	67.5 ± 7.2	-	0.014$	0.009#	0.033#	0.396#

291 * Determined by χ^2 test according to each group's male/female proportions. $ Determined by Kruskal-Wallis rank
292 sum test to compare age between all groups. # Determined by Dunn's test (Benjamini-Hochberg correction) to
293 compare age between group pairs. Diseases refer to AD and PD grouped together.

294 A total of 203 and 186 proteins were quantified in whole serum and HMW serum, respectively (Figure
295 2a, solid lines; Additional File 2: Supplementary Tables 1 and 2 for detailed information). A large overlap
296 was observed between both sample preparation procedures (168 proteins were shared, which
297 corresponds to more than 70% of all the quantified proteins). Additionally, quantification in the whole
298 serum of the proteins identified in the HMW serum library did not lead to a discernible increase in
299 proteome coverage (Figure 2a, dashed line; Additional File 2: Supplementary Table 3). Altogether, these

300 results indicate that there are no major differences in terms of the proteins being quantified in the two
301 approaches, revealing that the main aim of the HMW fractionation presented in this work –
302 fractionation under non-denaturing condition – is not the overall improvement of the proteome
303 coverage but the possibility of interrogating the samples considering protein
304 interactions/macromolecular organization.

305 This was further confirmed by the fact that only 14.7% of all the proteins considered altered in this study
306 (11 out of 69 proteins) were consistently altered in the fractionated and unfractionated samples (Figure
307 2b; Additional File 2: Supplementary Tables 1-2). Moreover, taking into consideration the changes of
308 those 11 commonly altered proteins, it is possible to observe that all proteins, except for the protein
309 beta-2-glycoprotein 1 (Figure 2c, bold), presented the same tendency in both fractionated and
310 unfractionated samples (Figure 2c). These results, in combination with the previous observations,
311 demonstrate that, although the two approaches quantified the same set of proteins, each method
312 interrogated the samples in a particular context, resulting in the identification of a different set of
313 altered proteins and the possibility to identify different regulatory mechanisms: while the direct analysis
314 of the serum mainly represents the alteration at the protein level, the HMW fractionation under non-
315 denaturing conditions may allow the evaluation of the physical interaction of the proteins.

316 These results are further supported by the analysis of the MW distribution of the proteins being studied,
317 which reveals a similar profile between both approaches (Additional File 1: Supplementary Figure 4a, 4b,
318 and 4c), with most of the proteins detected in HMW serum presenting a MW below 150 kDa. Moreover,
319 a similar distribution is observed for the proteins altered exclusively in the HMW approach (Additional
320 File 1: Supplementary Figure 4d), indicating that this strategy is not biased towards only the HMW
321 proteins and supporting the idea that those proteins altered in this fraction may correspond to proteins
322 being organized into different complexes.

323 **High molecular weight fractionation revealed differences in the macromolecular organization of the**
324 **serum proteome**

325 To test the hypothesis that the HMW approach is capable of evaluating the re-organization of protein
326 complexes, the nature of the 28 proteins altered exclusively in HMW serum was evaluated. This analysis

327 revealed that most of those proteins had been described to interact physically either with each other or
328 with other proteins (Figure 3a). Upon immediate observation of the GeneMania network, which
329 primarily evaluates the interactions between the proteins under study (Additional File 2: Supplementary
330 Table 4), it becomes apparent that the majority of the proteins participate in established physical
331 interactions. Moreover, it can be observed that these proteins form a large and interconnected network
332 comprising 20 of the 28 altered proteins centered around the interactions between the apolipoproteins
333 and lecithin-cholesterol acyltransferase (encoded by the *LCAT* gene). Although not participating in any
334 known interactions with another protein from the 28 altered proteins, the proteins Glutathione
335 peroxidase 3 (*GPX3*), Pigment epithelium-derived factor (*SERPINF1*), Thyroxine-binding globulin
336 (*SERPINA7*), and Alpha-1B-glycoprotein (*A1BG*) are also known to establish physical interactions
337 including with the proteins identified in this analysis. Only four of the 28 altered proteins, namely SRR1-
338 like protein (*SRRD*), carnosine dipeptidase 1 (*CNDP1*), peptidoglycan recognition protein 2 (*PGLYRP2*),
339 and serum amyloid A-4 protein (*SAA4*), were found to have no disclosed interactions in this particular
340 analysis. However, interactors for those proteins have already been pointed out in some screening
341 assays, as confirmed in BioGRID (Biological General Repository for Interaction Datasets, Additional File 2:
342 Supplementary Table 5). Furthermore, as revealed by the functional analysis, several of these 28
343 proteins are involved in the formation of complexes with lipids and platelet components (Additional File
344 2: Supplementary Table 6), indicating that those proteins can form complexes not only via the
345 interaction with other proteins but also with other molecules, and thus be organized in large complexes.
346 This involvement in the potential formation of macromolecular complexes is even more evident when
347 the functional pathways enriched in each of the two lists of proteins (30 and 28 altered proteins
348 exclusively in the whole serum or HMW serum, respectively) are directly compared (Figure 3b). This
349 comparison highlights the fact that all the pathways that are either only, or at least more, enriched in
350 the HMW dataset in comparison to the whole serum dataset (pathways indicated in bold) are related to
351 the formation/regulation of large complexes/macrostructures, namely amyloids, fibrin clot formation
352 and dissolution pathways and lipoprotein-related metabolism. On the other hand, the pathways that are
353 particularly enriched or unique in the whole serum dataset are mainly related to transcription factor
354 networks (Additional File 2: Supplementary Table 7).

355 **Evaluation of the potential of this combined strategy for biomarker discovery**

356 The previous set of results demonstrates that both approaches can provide complementary information.
357 In line with this evidence, the potential to use this combined strategy for biomarker discovery was also
358 evaluated. In general, both approaches result in nearly 40 proteins altered in at least one pair of
359 comparisons (Figure 4a-b; Additional File 1: Supplementary Figure 3 for details regarding each pair of
360 comparisons), with a tendency to have more proteins altered in the comparisons involving the AD group
361 (at least 20 proteins were altered compared to CT against a maximum of 14 altered proteins in PD vs.
362 CT, Additional File 1: Supplementary Figure 2a-b) and only a small subset of proteins altered in only one
363 comparison (15/41 in the whole serum and 11/39 in HMW serum, Figure 4a and 4b, respectively).
364 Besides those similarities, different profiles of altered proteins were observed depending on the
365 approach used. Hence, it can also be highlighted that while the whole serum strategy (Figure 4a) mainly
366 found proteins altered between the two disease groups (39 proteins in AD vs. PD compared to 20 and 12
367 proteins in AD vs. CT and PD vs. CT, respectively), the HMW approach (Figure 4b) captured more
368 differences between AD and CT samples (36 out of the 39 altered proteins). Due to this
369 complementarity, the combination of results from both approaches resulted in a more comprehensive
370 profile (Additional File 1: Supplementary Figure 2a-c), with a general increase in the number of altered
371 proteins per group (total of 69 altered proteins, Figure 4c). This improvement is particularly evident in
372 the case of proteins altered between PD and CT samples, for which only one protein was considered
373 commonly altered in the two approaches (Figure 2c and Additional File 1: Supplementary Figure 2b),
374 thus resulting in the duplication of the list of proteins with the potential to serve as biomarkers for PD
375 versus CT individuals. Common to all mapped profiles was the low number of proteins altered between
376 all three groups (4, 1, and 6 for Whole serum, HMW serum and the combination of both, Figure 4a-c,
377 respectively) and the absence of proteins altered exclusively between PD and CT samples.

378 To further confirm the biomarker potential of the altered proteins from the three strategies presented
379 above, they were used as input to build discriminant models that could differentiate between the
380 studied groups (Figure 4d-f). From each dataset, candidates whose combination resulted in the best
381 possible discriminant model were automatically selected (detailed information regarding the methods in
382 Table 2), resulting in three distinct and statistically valid models (all with $p < 0.0032$) capable of

383 discriminating the three groups being studied. The whole serum dataset resulted in a reasonable model
384 composed of 4 proteins (Figure 4d), with a median sensitivity (the capacity to classify the individuals
385 from each disease group correctly) of 86.95% (sensitivity and specificity are summarized in Additional
386 File 1: Supplementary Table 8). On the other hand, the model created with six proteins from the HMW
387 approach (Figure 4e) had lower performance, with a median sensitivity of only 80.3% (corresponding to
388 83.3% predicting capacity for PD samples and 77.3% for AD samples). Moreover, neither of the models
389 was particularly good in the classification of CT samples, resulting in a specificity of only 66.7% and 75%
390 in the whole serum and HMW serum models, respectively. Remarkably, the combined model (created
391 from the dataset containing the altered proteins from both approaches - Figure 4f) clearly outperformed
392 the two models based only on proteins from a single approach. For this combined model, 10 proteins
393 were selected and integrated, creating a discriminant model capable of correctly classifying more than
394 96% of all tested samples (93% in a cross-validation test; Table 2). This included the correct classification
395 of 100% of samples from the PD group (Figure 4f), which encompassed samples from younger patients
396 compared to the other studied groups (Table 1). However, it was confirmed that this age difference did
397 not interfere with the classification of samples when employing the discriminant model since: i) age by
398 itself did not yield good classification performance (Additional File 1: Supplementary Figure 5) and ii)
399 none of the 10 proteins included in the combined model were strongly correlated with age (Additional
400 File 1: Supplementary Figure 6). Altogether, this combined method presented a median sensitivity of
401 97.75% and a specificity of 91.7%.

402 The diagnostic capacity of these models was further assessed by ROC curves, which measured their
403 ability to accurately classify AD and PD patients from among all other samples (Figure 4g-i). This analysis
404 confirmed that the best model is the one created with the combination of proteins from both
405 approaches and that, in general, the model using only proteins from the whole serum approach is better
406 than the model from the HMW approach. The respective statistics (Figure 4i) further support that the
407 whole serum model performed better than the HMW serum model but without statistically significant
408 differences between the two ROC curves. Additionally, the statistical analysis also confirmed that the
409 combined model (AUC = 0.999 for the classification of AD and PD patients) is the best model and that it
410 performed significantly better ($p < 0.05$) than both other models for PD classification (HMW serum, AUC

411 = 0.888; whole serum, AUC = 0.960) and better than the HMW serum model (AUC = 0.919) in the case of
412 AD classification. The robustness of the combined model is further evidenced by the confidence interval
413 (CI) of the AUC, which has a lower limit above 0.93 for both diseases, in contrast with the values
414 achieved for the other two methods, whose lower limits are all below 0.9.

415 **Table 2.** Linear Discriminant models, respective statistical analysis and classification results.

	Gene Name	Protein name	MW (KDa)	Whole Serum Dis 1	Whole Serum Dis 2	HMW serum Dis 1	HMW serum Dis 2	Whole + HMW serum Dis 1	Whole + HMW serum Dis 2
#	***FOXM1***	**Forkhead box protein M1**	**84.283**	---	---	---	---	**245.36**	**-10.93**
#	*PROC*	Vitamin K-dependent protein C	52.071	-1133.77	1212.34	---	---	-1557.39	623.28
#	*HBB*	Hemoglobin subunit beta (Beta-globin)	15.998	1.49	0.58	-0.06	-0.13	0.42	-1.50
#	*APOA1*	Apolipoprotein A1 (Apo-AI)	30.778	3.63	0.53	---	---	-0.16	-3.08
#	***IGLV3-19***	**Immunoglobulin lambda variable 3-19**	**12.042**	---	---	---	---	**62.89**	**52.70**
§	*SRRD*	SRR1-like protein	38.573	---	---	20.37	7.55	16.69	11.52
§	*APOC1*	Apolipoprotein C1 (Apo-CI)	9.332	---	---	-9.74	19.21	-15.77	1.33
§	*APOE*	Apolipoprotein E (Apo-E)	36.154	---	---	1.46	-0.42	0.84	0.53
§	***SERPINF1***	**Pigment epithelium-derived factor (PEDF)**	**46.312**	---	---	---	---	**6.85**	**2.63**
§	*KRT9*	Keratin, type I cytoskeletal 9	62.064	---	---	-8.80	5.05	-12.73	-4.91
	PPBP	**Platelet basic protein (PBP)**	**13.894**	---	---	**8.89**	**-7.88**	---	---
	TF	**Serotransferrin (Transferrin)**	**77.050**	**-0.99**	**-1.66**	---	---	---	---
		(Constant)		2.11	-0.81	-1.11	-2.82	3.34	-1.10
	Statistics (Wilks' Lambda, Chi-square and p-value)		**λ=**	0.253	0.773	0.242	0.629	0.058	0.292
			χ2=	73.473	13.473	74.458	24.361	143.675	62.244
			p<	9.97×10^{-13}	3.23×10^{-03}	4.65×10^{-11}	1.85×10^{-04}	1.01×10^{-20}	4.94×10^{-10}
	Overall classification results (% of cases correctly classified)		**Original**	82.8		79.3		96.6	
			Cross-validation	81.0		72.4		93.1	

416 # selected from the data from the whole serum approach for the Whole + HMW serum model; § selected from the data from the HMW serum approach for the Whole + HMW serum model;

417 Dis – discriminant function; Note that proteins are sorted by order of inclusion into the Whole + HMW serum discriminant model.

418 By looking at the proteins selected to build the different methods (Table 2), it was observed that the
419 combined method is not the simple combination of the proteins previously selected from each of the
420 individual methods. The combined model is built by the combination of 10 proteins, five from each
421 dataset, including three [forkhead box protein M1 (*FOXM1*), immunoglobulin lambda variable 3-19
422 (*IGLV3-19*) and pigment epithelium-derived factor (*SERPINF1*)] that were not selected on the database-
423 specific models. On the other hand, some previously selected proteins [serotransferrin (*TF*) and platelet
424 basic protein (*PPBP*)] were not included in the combined model. Finally, the Hemoglobin subunit beta
425 (*HBB*) was selected in both approach-specific models, although only data from the whole serum dataset
426 was used in the combined model. These results demonstrate that the increase in the initial amount of
427 data provided for the discriminant analysis has an important impact on the generated model by making
428 it possible to test different combinations of proteins and, thus, allowing for the identification of better
429 combinations than those highlighted in the analysis of individual datasets. Interestingly, all ten proteins
430 selected in the combined model have a MW below 90 kDa (Table 2). This finding confirms that all the
431 proteins selected from the HMW approach have a MW below the theoretical cut-off of the filters used
432 for fractionation. This observation supports the hypothesis that this approach might effectively assess
433 the remodeling of molecular complexes. By plotting the individual values of each of the ten proteins
434 selected in the combined model (Figure 5a), it is possible to observe that, as expected, those values
435 present some variation characteristic of the individuality of each patient. Nevertheless, considering that
436 the model was able to correctly classify more than 90% of all the patients (Figure 4f), it is possible to
437 infer that the combinations performed in the model could diminish the impact of the biological
438 variability, proving that the combination of different markers can overcome their individual weaknesses.
439 The analysis of these results immediately reveals that i) only three proteins from the model (the
440 proteins encoded by the genes *FOXM1, HBB,* and *SRRD*) are significantly altered between all three
441 groups and ii) only one protein, the apolipoprotein C1 (Apo-CI, encoded by the *APOC1* gene), is altered
442 between a single comparison, in this case between AD and PD which may indicate that this protein may
443 have a particularly important role in this model for distinguishing AD from PD patients. Among the
444 remaining 6 proteins: i) three, apolipoprotein E, pigment epithelium-derived factor and KRT9, are
445 altered between both disease groups and control sample (all three found in the HMW fraction); ii) two,
446 apolipoprotein A1 and immunoglobulin lambda variable 3-19, are altered in AD in comparison to both

447 PD and CT, and one, the Vitamin K-dependent protein C (encoded by the PROC gene), is altered in PD
448 patients in comparison to the other two groups. Moreover, it is noteworthy that while there was a
449 tendency to incorporate proteins that were increased in AD compared to CT from the whole serum
450 approach (three out of the five proteins from the whole serum model, encoded by the genes *FOXM1,*
451 *HBB,* and *APOA1*), the opposite trend was observed in the case of proteins from the HMW approach.
452 Specifically, three out of the five proteins (the proteins encoded by the genes *SRRD, APOE,* and
453 *SERPINF1*) were found to be decreased in the AD vs. CT comparison. On the contrary, for the PD vs. CT
454 comparison, there were no major differences in terms of tendencies when considering the proteins
455 captured in the whole serum or the HMW serum.

456 Finally, all proteins from the whole serum dataset, in addition to SRR1-like protein (encoded by the
457 *SRRD* gene) and Apo-CI from the HMW dataset, were significantly altered between both disease groups.
458 From these, three proteins [the protein Forkhead box protein M1 (encoded by the *FOXM1* gene),
459 hemoglobin subunit beta (encoded by *HBB* gene), and apolipoprotein A1 (Apo-AI, encoded by the
460 *APOA1* gene)] are less abundant in PD samples than in AD samples, while the remaining four are
461 increased.

462 The correlation analysis of the protein abundances among groups confirmed that, in general, there is no
463 particularly evident correlation between the profiles and the magnitude of regulation of these proteins
464 (Figure 5b). There were, however, some observed exceptions, including a strong positive correlation
465 between the proteins encoded by the genes *APOA1* and *FOXM1* (r = 0.8) and, to a lesser extent, the
466 proteins encoded by *APOC1, APOE and SERPINF1* (r = 0.5-0.6). Interestingly, the proteins showing a
467 positive correlation originated from the same approach, the gene products of *APOA1* and *FOXM1* were
468 both highlighted in the whole serum approach, suggesting that the overall levels of these two proteins
469 were similarly altered. Meanwhile, the products of the *APOC1, APOE,* and *SERPINF1* genes were
470 identified as altered in the HMW fractionation strategy, which may indicate that these proteins might be
471 part of the same complex and thus regulated in a similar manner. No remarkable negative correlations
472 were found, with the strongest correlation observed between the proteins encoded by the *APOA1* and
473 *SRRD* genes, which indicates that none of the proteins in the model present a completely opposite
474 regulation profile. Additionally, an unsupervised clustering analysis using these ten proteins (Figure 5c)

475 confirmed their capacity to partially distinguish the three groups being studied, revealing that, besides
476 the existence of individual variability, it was possible to identify three independent clusters composed
477 exclusively or mainly of samples from one of the three groups. This analysis also demonstrates that this
478 set of proteins is particularly efficient in isolating the AD patients from the remaining individuals from
479 the study: the AD cluster was composed exclusively of AD patients, and only 6 out of the 22 AD patients
480 were not included in this cluster. On the other hand, a slightly lower separation capacity was observed
481 for both PD and CT samples. These two clusters contained few samples that did not belong to their
482 respective groups, resulting in a higher percentage of individuals not properly grouped (10 out of 24 and
483 4 out of 12 samples for PD and CT, respectively). The discrepancies observed between the clustering
484 analysis and the discriminant model results, where the latter correctly classified over 90% of the
485 samples, can be attributed to the fact that the clustering analysis relied solely on the individual protein
486 distribution profiles across the samples. In contrast, the discriminant analysis employed equations with
487 different weightings for each protein, resulting in a single model that effectively reduces the intragroup
488 variability while promoting a better separation between the analyzed groups. Despite that, the
489 clustering analysis remains an important approach for understanding how the proteins are modulated
490 within the samples. Thus, from the three different clusters highlighted in the analysis, it was possible to
491 infer the median protein abundance profile of these proteins among the three groups. For instance, the
492 gene products of *SERPINF1, APOE* and *APOC1* tend to be less abundant in both disease groups compared
493 to CT samples. Furthermore, some proteins are more abundant in each disease group, namely the gene
494 products of *PROC* and *KRT9* in PD samples and the gene products of *HBB, APOA1* and *FOXM1* in AD
495 samples. Another disease-specific observation was the smaller amount of immunoglobulin lambda
496 variable 3-19 (*IGLV3-19*) in AD samples compared to both other groups. Overall, these tendencies
497 characterize the unique profiles determined for each disease group, which may be a precursor to a
498 potential future biomarker panel that could be more informative than the analysis based on any single
499 protein.

500 Finally, STRING analysis (Figure 5d and Additional File 2: Supplementary Table 9) revealed that these ten
501 proteins have more interactions among themselves than what would be expected for a random set of
502 proteins of the same size and degree of distribution, indicating that this set of proteins is, at least

503 partially, biologically connected (PPI enrichment $p = 2.07\times10^{-5}$). This result may be mainly due to the
504 strong network involving apolipoproteins and Hemoglobin subunit beta (cluster 1). Again, two out of the
505 ten proteins selected for the discriminant method revealed to be associated with high-density
506 lipoproteins (HDL) and chylomicron (ultra-low-density lipoproteins particles) remodeling and assembly
507 (Figure 5e and Additional File 2: Supplementary Table 10), highlighting the potential importance of these
508 mechanisms in the neurodegenerative process, and confirming that the proteins related with these
509 mechanisms could be good biomarker candidates for their diagnosis.

510 Given the central role that apolipoproteins appear to play in this model, a discriminant analysis was
511 performed using data from ten altered proteins involved in apolipoprotein-related mechanisms to
512 investigate if the diagnostic model could be limited to this set of functionally related proteins (Additional
513 File 1: Supplementary Figure 7). However, the generated model exhibited lower diagnostic capacity
514 compared to the combined approach, with only 82.75% of the samples being correctly classified. The
515 model demonstrated a specificity of 66.7%, and a sensitivity of 86.4% and 87.5% for AD and PD,
516 respectively, yielding ROC curves with AUCs equal to or below 0.955. Thus, besides the importance of
517 apolipoproteins, the results from these proteins alone are not enough to distinguish the three groups,
518 emphasizing the importance of having diagnostic models based on several complementary candidates
519 instead of a single or just a few candidates. Nonetheless, the identification of this robust core of
520 functionally related proteins underscores the significance of the combined approach for identifying new
521 potential biomarkers. For instance, while the dysregulation of Apo-C1 and Apolipoprotein E (Apo-E,
522 encoded by the *APOE* gene) was discovered using the HMW fractionation approach, the dysregulation of
523 Apo-AI was identified using the whole serum approach.

524

525 ## Discussion

526 The present study presents a proof of concept of a novel two-pronged approach to biomarker discovery
527 in complex peripheral biological fluids. More specifically, it was demonstrated that through the
528 combination of two complementary proteomics strategies, the direct analysis of whole serum and the
529 analysis of serum HMW fraction (above 300 kDa) in non-denaturing conditions, another level of
530 proteome characterization of the samples could be achieved. This resulted in more robust diagnostic
531 models and insights into disease mechanisms. In this sense, when applied to serum samples from a
532 cohort of control individuals and individuals afflicted by neurodegenerative diseases, this strategy
533 allowed for a strong discriminant model to be built, able to distinguish all studied groups more
534 effectively than the models generated from a single proteomics analysis. The most noticeable findings
535 from this model showed that several, otherwise overlooked, proteins may yet serve as potential
536 biomarkers of disease, in this case, AD and PD, particularly when analyzed together in a model created
537 using the two different approaches. Thus, these results confirm the importance of having a panel of
538 potential candidates rather than a single protein biomarker. Furthermore, they also demonstrate that
539 the biomarker discovery field will benefit from combining data from the sample obtained through
540 different sample processing strategies. While not individually sufficient to be considered as biomarkers,
541 the significant influence of apolipoproteins, particularly Apo-AI, Apo-CI, and Apo-E, in the
542 aforementioned discriminant model, suggests a potential disease-specific dysregulation of lipoprotein
543 metabolism in AD and PD patients.

544 **High molecular weight fractionation may reveal a potentially altered macromolecular and**
545 **macromolecular-complex organization**

546 In this work, it was demonstrated that interrogating serum samples with the HMW fractionation
547 method adds an extra layer of information capable of bringing new insight into the behavior of the
548 serum proteins, particularly regarding their potential macromolecular organization. Because the
549 fractionation procedure took place under non-denaturing conditions and since aberrant protein
550 aggregation [8] is a common hallmark of both AD and PD, it was hypothesized that macromolecular

551 complexes, potentially altered between the studied groups, could be captured through the HMW
552 fractionation approach.

553 The present results confirmed this premise, as evidenced by the fact that although no variation was
554 observed in the overall serum protein captured by both strategies, proteins exclusively altered in the
555 HMW fraction accounted for 40% of the total list of altered proteins. Furthermore, with the exception of
556 one protein (Centrosome-associated protein CEP250), all proteins had a MW below 90 kDa, which is
557 considerably lower than the 300 kDa cut-off filter used. It is worth noting that 72% of proteins altered in
558 the HMW fraction did not exhibit alterations in their total levels. This supports the possibility that
559 different regulatory mechanisms of these proteins, apart from expression and degradation, are being
560 revealed and studied using this approach.

561 Moreover, the results show that most of these proteins have several reported interactors and thus may
562 be involved in the formation of large complexes. An illustration of this phenomenon is found in the
563 protein clusterin (CLU gene), also known as apolipoprotein J, which has been implicated in the
564 metabolism of aggregation-prone proteins, including those associated with NDs [31-33]. Notably,
565 clusterin's interaction with Aβ42 has been demonstrated to enhance its clearance from the brain
566 through the blood-brain barrier (BBB) [31]. Furthermore, clusterin has been implicated in various stages
567 of PD, potentially exerting a neuroprotective effect through its interaction with α-synuclein aggregates
568 [32]. Additionally, the interaction between clusterin and α-synuclein has been detected in plasma
569 samples [33]. Beyond this specific example, the generic functional analysis of altered proteins,
570 particularly those from the HMW serum strategy, suggests their close association with amyloids and clot
571 formation, which may involve large structures.

572 On the other hand, some of these proteins may instead, or additionally, be present in large biological
573 structures not composed exclusively of proteins, like exosomes or lipoproteins, which would not only
574 likewise justify their presence in this HMW serum fraction but also give further understanding of the
575 potentially altered mechanisms related to the diseases being studied. Such may be the case of the
576 proteins clusterin and serum amyloid A-4 (*SAA4* gene), which were found to be altered in serum neuron-
577 derived exosomes of AD patients [34]. Additionally, exosomal clusterin was found to be altered in

578 patients at different stages of PD when compared to controls [35]. Thus, although the presence of
579 exosomes in the HMW fraction was not confirmed, given the MWCO of the filters used in this work, it is
580 feasible that some of the proteins being analyzed in the HMW fraction may correspond to proteins
581 linked to the extracellular vesicles.

582 Altogether, these findings support the notion that the HMW fractionation approach can provide a new
583 level of information that may offer new insights into how proteins are organized within a given sample.

584 **Altered lipoprotein metabolism can be a peripherical marker of AD and PD**

585 The combination of the two approaches in this study led to a robust and promising potential biomarker
586 panel composed of ten proteins quantified in whole serum or HMW serum. A major finding revealed by
587 this model was the involvement of several lipoproteins in discriminating between the studied groups.
588 Among the ten proteins used in the best discriminant model, three are apolipoproteins: Apo-AI from
589 whole serum, and Apo-CI and Apo-E from HMW serum. Besides those three proteins, other altered
590 apolipoproteins were observed in this study but not included in the model, namely: i) the Apo-AII, Apo-
591 LI and clusterin highlighted in the HMW serum strategy; ii) the Apo-AIV from the whole serum; and, iii)
592 beta-2-glycoprotein 1 in both approaches. Furthermore, a lipoprotein-related enzyme, lecithin-
593 cholesterol acyltransferase, was also altered in HMW serum. This is further supported by the functional
594 enrichment analysis of the altered proteins discovered in both strategies that highlight the involvement
595 of those proteins in lipoprotein metabolism and HDL-mediated lipid transport pathways. Cumulatively,
596 all these findings point to the relevance of lipoproteins in the context of NDs and, although not
597 absolutely clear, the link between these diseases, in particularly AD, and apolipoproteins has been the
598 focus of many studies [31, 33, 36-46].

599 Apo-AI and Apo-E have an established relation to toxic species clearance from the brain in AD and PD
600 [31, 33, 37, 47-50]. Additionally, regarding AD, our findings for both proteins contradict what can be
601 found in the literature [38, 43]. For Apo-AI, we found an increase in abundance in AD patients as
602 opposed to the decrease reported for most studies [38]. However, in another study where no significant
603 alterations in total serum Apo-AI content of AD patients were reported, further investigation revealed
604 that some proteoforms of this protein were significantly increased compared to the levels observed in

605 the controls [39]. This has been suggested as a possible explanation for the different observations
606 regarding this protein in the context of AD, which might be related to the use of different detection
607 methods within different studies [38]. Regarding this protein's connection to clearance mechanisms,
608 evidence suggests that for HDLs containing Apo-AI (APOA1-HDL), the structure seems to influence not
609 only the disaggregation of Aβ fibrils but also its ability to cross the BBB, with lipid-poor discoidal APOA1-
610 HDL having the best performance when compared to APOA1-HDL in other lipidation states [37].
611 Moreover, in the present study, phosphatidylcholine-sterol acyltransferase, an enzyme known to affect
612 HDL structure through lipidation of Apo-AI in plasma [45], was also found to be altered in AD patients.
613 As this enzyme participates in HDL maturation in plasma [51], this result could reflect the dysregulation
614 of lipoproteins in AD. For Apo-E, we found a decrease in abundance in AD patients as opposed to the
615 increase reported for MCI patients in a previous study [43]. Isoform and lipidation status of Apo-E is also
616 crucial for the Aβ clearance, with the Apo-E4 isoform, the genetic risk factor most associated with the
617 onset of AD [31, 48], and higher lipidation having detrimental effects on the process [31, 48]. Further
618 investigation using the combined approach presented in this study, particularly in the context of AD,
619 should also involve a lipid profile analysis and APOE genotyping of the participants to enable a more
620 comprehensive characterization of serum HDLs and Apo-E content, respectively.

621 Although systemic lipid abnormalities have also been implicated in PD, there are fewer findings
622 connecting it to HDL-related proteins, as compared to AD [32]. Nonetheless, a previous report observed
623 significantly decreased values of Apo-AI in mild PD patients compared to healthy controls, but much like
624 what we observed for this protein, a less impactful and non-significant decrease was observed in
625 moderate/severe PD patients [52]. In fact, most research indicates that Apo-AI may have a protective
626 role in PD [32] and it has been hypothesized that APOA1-HDL could take part in the efflux of α-synuclein
627 from the brain [33]. Additionally, both Apo-AI and Apo-E have been reported to interact with α-
628 synuclein [33].

629 Finally, HDL size and plasma levels have been shown to be dependent on the levels of Apo-CI [53],
630 another apolipoprotein included in the best diagnostic model generated in this study. Besides that, a
631 previous study also shows that the dysregulation of this protein can lead to impaired memory processes
632 in mice [54]. This suggests that the regulation of Apo-CI can be pivotal in the brain and that a systemic

633 disruption of this process could have effects detectable beyond the CNS, particularly in lipoprotein
634 metabolism, that could be observable in peripheral biofluids. Interestingly, this study found that Apo-CI
635 significantly decreased in the HMW serum fraction of AD compared to PD patients, but only a slight and
636 non-significant decrease was observed when compared to CT patients. Similarly, only a small non-
637 significant decrease in HMW serum Apo-CI was observed for controls in comparison to PD patients,
638 which is in accordance to what was already reported for whole plasma [40]. Given that memory
639 impairment is a hallmark of AD and not a predominant feature among PD patients [55], these results
640 may be influenced, at least in part, by the age disparities observed between the PD group and the other
641 two groups. In fact, PD patients are, on average, younger than those in the other two groups, with
642 similar age distributions. Additionally, the results regarding Apo-CI may also be affected by individual
643 Apo-CI and Apo-E isoforms. Notably, the *APOE* and *APOC1* genes are in linkage disequilibrium [56], and
644 carriers of the *APOE(ε4)* and *APOC1(H2)* alleles have been demonstrated to have an increased risk of
645 developing AD [46]. This was further confirmed in a study using human *APOE*-carrying mice, which
646 demonstrated that those animals carrying the *APOE(ε4)* allele were found to have decreased serum
647 Apo-CI content when compared to those carrying the *APOE(ε3)* allele [57]. However, Apo-CI has also
648 been suggested to potentially play a modulatory role in the development of AD, with reported effects
649 on mice cognitive function independent of Apo-E expression [58]. Again, these observations strengthen
650 the importance of combining these results with further characterization of the individuals, including
651 genotyping of the apolipoproteins' isoforms.

652 Although these three apolipoproteins have been linked to AD and PD, as evidenced by previously
653 mentioned studies, and their relevance for the discriminant model, their use alone or in combination
654 with other proteins associated with apolipoprotein-related mechanisms did not result in a robust
655 diagnostic model capable of effectively distinguishing between the studied groups (as shown in
656 Additional File 1: Supplementary Figure 7). This indicates that these three apolipoproteins had to be
657 combined with other seemingly unrelated proteins to be used as potential biomarkers. Further studies
658 should be directed towards elucidating this potential relationship to understand: i) the importance of
659 the identified proteins/mechanisms for the pathophysiology of the studied NDs, and ii) to which extent
660 these mechanisms are differently altered between the two diseases.

661 In summary, this work demonstrated that combining two complementary sample processing
662 approaches is a more effective strategy to reach potential biomarkers than a single approach. Besides
663 that, the strategies used here, which combine the analysis of the whole serum and the HMW
664 fractionation of non- denaturing serum, can also identify proteins being differentially modulated besides
665 the conventional alteration in their total levels. In this work, this new strategy was applied to a cohort of
666 NDs patients and respective CT individuals, being able to build a good predictive model capable of
667 distinguishing all the three groups studied (AD, PD and CT). This predictive model highlighted the linkage
668 of the apolipoprotein family and NDs, with three out of the ten proteins included in this model being
669 apolipoproteins. Nevertheless, further validation in a larger and independent cohort is needed to
670 confirm the robustness and reliability of the model, as well as more studies to link the alterations
671 observed and these pathologies. Controlling the lipid profile in future studies is also advised, as altered
672 lipid metabolism was a major finding of the present work. Another aspect to be further explored would
673 be the identification of protein complexes in the HMW fraction to better understand the origin of the
674 protein alterations observed.

675 Overall, the results of this study demonstrate that HMW fractionation under non-denaturing conditions
676 could be a valuable addition to routine biofluid analysis, particularly regarding the detection of changes
677 in macromolecular organization. Furthermore, this study highlights the importance of exploring the
678 involvement of apolipoproteins and lipid metabolism in greater detail within the context of NDs.

679

Acknowledgements

All authors have read the journal's authorship statement. The authors would like to thank the financial support of the European Regional Development Fund (ERDF), through the COMPETE 2020 - Operational Programme for Competitiveness and Internationalisation and Portuguese national funds via FCT – Fundação para a Ciência e a Tecnologia, I.P., under projects: MEDPersyst - POCI-01-0145-FEDER-016428 (ref.: SAICTPAC/0010/2015), POCI-01-0145-FEDER-30943 (ref.: PTDC/MEC-PSQ/30943/2017), PTDC/MED-NEU/27946/2017, POCI-01-0145-FEDER-016795 (ref.: PTDC/NEU-SCC/7051/2014), POCI-01-0145-FEDER-029311 (ref.: PTDC/BTM-TEC/29311/2017); EXPL/BTM-TEC/1407/2021, and, UIDB/04539/2020, UIDP/04539/2020, UIDB&P/4950/2020 and LA/P/0058/2020, and the National Mass Spectrometry Network (RNEM) [POCI-01-0145-FEDER-402-022125 Ref. ROTEIRO/0028/2013). SIA was supported by the CEEC grant 2021.04378.CEECIND and MR was supported by Ph.D. fellowship 2020.07749.BD.

Ethics approval

The study was approved by the Ethics Committee of the Faculty of Medicine of the University of Coimbra (reference CE_010.2017) and the Ethics Committee of the Centro Hospitalar e Universitário de Coimbra (CHUC) (reference 34 /CES-CHUC-024-18) and was conducted according to the principles stated in the Declaration of Helsinki [59]. Written informed consent was obtained from all participants.

Data linking

The MS proteomics data have been deposited to the ProteomeXchange Consortium [60] via the PRIDE [61] partner repository with the dataset identifier PXD034077 (for reviewer: Username: reviewer_pxd034077@ebi.ac.uk; Password: jhF8zQaR).

Competing interests

The authors declare that they have no competing interests

Authors' contributions

SIA and BM conceived and designed the study. SIA and MR performed all the experiments, data analysis, and wrote the manuscript. IB, AG, DP, CS, JP, CJ, IS, AV, AM, and MCB were involved in the selection and collection of the plasma samples used in this study. MCB and BM were responsible for funding. The author(s) read and approved the final manuscript.

708 **References**

709 [1] Anderson NL, Anderson NG. The Human Plasma Proteome: History, Character, and Diagnostic
710 Prospects*. Molecular & Cellular Proteomics. 2002;1:845-67.

711 [2] Antoranz A, Sakellaropoulos T, Saez-Rodriguez J, Alexopoulos LG. Mechanism-based biomarker
712 discovery. Drug Discovery Today. 2017;22:1209-15.

713 [3] Anjo SI, Santa C, Manadas B. SWATH-MS as a tool for biomarker discovery: From basic research to
714 clinical applications. PROTEOMICS. 2017;17:1600278.

715 [4] Anjo SI, Manadas B. A translational view of cells' secretome analysis - from untargeted proteomics to
716 potential circulating biomarkers. Biochimie. 2018;155:37-49.

717 [5] Rosado M, Silva R, G. Bexiga M, G. Jones J, Manadas B, Anjo SI. Chapter Four - Advances in biomarker
718 detection: Alternative approaches for blood-based biomarker detection. In: Makowski GS, editor.
719 Advances in Clinical Chemistry: Elsevier; 2019. p. 141-99.

720 [6] Greening DW, Simpson RJ. A centrifugal ultrafiltration strategy for isolating the low-molecular weight
721 (≤25K) component of human plasma proteome. Journal of Proteomics. 2010;73:637-48.

722 [7] Greening DW, Simpson RJ. Low-Molecular Weight Plasma Proteome Analysis Using Centrifugal
723 Ultrafiltration. In: Simpson RJ, Greening DW, editors. Serum/Plasma Proteomics: Methods and
724 Protocols. Totowa, NJ: Humana Press; 2011. p. 109-24.

725 [8] Espay AJ, Vizcarra JA, Marsili L, Lang AE, Simon DK, Merola A, et al. Revisiting protein aggregation as
726 pathogenic in sporadic Parkinson and Alzheimer diseases. Neurology. 2019;92:329-37.

727 [9] Hughes AJ, Daniel SE, Kilford L, Lees AJ. Accuracy of clinical diagnosis of idiopathic Parkinson's
728 disease: a clinico-pathological study of 100 cases. Journal of Neurology, Neurosurgery & Psychiatry.
729 1992;55:181-4.

730 [10] American Psychiatric Association A, Association AP. Diagnostic and statistical manual of mental
731 disorders: DSM-IV: American psychiatric association Washington, DC; 1994.

732 [11] McKhann GM, Knopman DS, Chertkow H, Hyman BT, Jack Jr CR, Kawas CH, et al. The diagnosis of
733 dementia due to Alzheimer’s disease: Recommendations from the National Institute on Aging-
734 Alzheimer’s Association workgroups on diagnostic guidelines for Alzheimer's disease. Alzheimer's &
735 dementia. 2011;7:263-9.

736 [12] Anjo SI, Simoes I, Castanheira P, Graos M, Manadas B. Use of recombinant proteins as a simple and
737 robust normalization method for untargeted proteomics screening: exhaustive performance
738 assessment. Talanta. 2019;205:120163.
739 [13] Anjo SI, Santa C, Manadas B. Short GeLC-SWATH: a fast and reliable quantitative approach for
740 proteomic screenings. Proteomics. 2015;15:757-62.
741 [14] Santa C, Anjo SI, Manadas B. Protein precipitation of diluted samples in SDS-containing buffer with
742 acetone leads to higher protein recovery and reproducibility in comparison with TCA/acetone approach.
743 Proteomics. 2016;16:1847-51.
744 [15] Anjo SI, Melo MN, Loureiro LR, Sabala L, Castanheira P, Grãos M, et al. oxSWATH: An integrative
745 method for a comprehensive redox-centered analysis combined with a generic differential proteomics
746 screening. Redox biology. 2019;22:101130.
747 [16] Gillet LC, Navarro P, Tate S, Röst H, Selevsek N, Reiter L, et al. Targeted data extraction of the
748 MS/MS spectra generated by data-independent acquisition: a new concept for consistent and accurate
749 proteome analysis. Molecular & Cellular Proteomics. 2012;11.
750 [17] Tang WH, Shilov IV, Seymour SL. Nonlinear fitting method for determining local false discovery rates
751 from decoy database searches. Journal of proteome research. 2008;7:3661-7.
752 [18] Sennels L, Bukowski-Wills JC, Rappsilber J. Improved results in proteomics by use of local and
753 peptide-class specific false discovery rates. BMC Bioinformatics. 2009;10:179.
754 [19] Lambert J-P, Ivosev G, Couzens AL, Larsen B, Taipale M, Lin Z-Y, et al. Mapping differential
755 interactomes by affinity purification coupled with data-independent mass spectrometry acquisition.
756 Nature methods. 2013.
757 [20] Collins BC, Gillet LC, Rosenberger G, Röst HL, Vichalkovski A, Gstaiger M, et al. Quantifying protein
758 interaction dynamics by SWATH mass spectrometry: application to the 14-3-3 system. Nature methods.
759 2013.
760 [21] MedCalc.
761 [22] DeLong ER, DeLong DM, Clarke-Pearson DL. Comparing the areas under two or more correlated
762 receiver operating characteristic curves: a nonparametric approach. Biometrics. 1988:837-45.
763 [23] MORPHEUS.

764 [24] Caraux G, Pinloche S. PermutMatrix: a graphical environment to arrange gene expression profiles in
765 optimal linear order. Bioinformatics. 2005;21:1280-1.
766 [25] PermutMatrix.
767 [26] Warde-Farley D, Donaldson SL, Comes O, Zuberi K, Badrawi R, Chao P, et al. The GeneMANIA
768 prediction server: biological network integration for gene prioritization and predicting gene function.
769 Nucleic Acids Research. 2010;38:W214-W20.
770 [27] GeneMANIA.
771 [28] STRING.
772 [29] Szklarczyk D, Morris JH, Cook H, Kuhn M, Wyder S, Simonovic M, et al. The STRING database in
773 2017: quality-controlled protein-protein association networks, made broadly accessible. Nucleic Acids
774 Res. 2017;45:D362-d8.
775 [30] Pathan M, Keerthikumar S, Ang CS, Gangoda L, Quek CY, Williamson NA, et al. FunRich: An open
776 access standalone functional enrichment and interaction network analysis tool. Proteomics.
777 2015;15:2597-601.
778 [31] Bell RD, Sagare AP, Friedman AE, Bedi GS, Holtzman DM, Deane R, et al. Transport pathways for
779 clearance of human Alzheimer's amyloid beta-peptide and apolipoproteins E and J in the mouse central
780 nervous system. Journal of cerebral blood flow and metabolism : official journal of the International
781 Society of Cerebral Blood Flow and Metabolism. 2007;27:909-18.
782 [32] Berdowska I, Matusiewicz M, Krzystek-Korpacka M. HDL Accessory Proteins in Parkinson's Disease—
783 Focusing on Clusterin (Apolipoprotein J) in Regard to Its Involvement in Pathology and Diagnostics—A
784 Review. Antioxidants. 2022;11.
785 [33] Emamzadeh FN, Allsop D. α-Synuclein Interacts with Lipoproteins in Plasma. Journal of Molecular
786 Neuroscience. 2017;63:165-72.
787 [34] Arioz BI, Tufekci KU, Olcum M, Durur DY, Akarlar BA, Ozlu N, et al. Proteome profiling of neuron-
788 derived exosomes in Alzheimer's disease reveals hemoglobin as a potential biomarker. Neuroscience
789 Letters. 2021;755:135914.
790 [35] Kitamura Y, Kojima M, Kurosawa T, Sasaki R, Ichihara S, Hiraku Y, et al. Proteomic Profiling of
791 Exosomal Proteins for Blood-based Biomarkers in Parkinson's Disease. Neuroscience. 2018;392:121-8.

792 [36] Berdowska I, Matusiewicz M, Krzystek-Korpacka M. HDL Accessory Proteins in Parkinson's Disease–
793 Focusing on Clusterin (Apolipoprotein J) in Regard to Its Involvement in Pathology and Diagnostics–A
794 Review. Antioxidants. 2022;11.
795 [37] Dal Magro R, Simonelli S, Cox A, Formicola B, Corti R, Cassina V, et al. The Extent of Human
796 Apolipoprotein A-I Lipidation Strongly Affects the β-Amyloid Efflux Across the Blood-Brain Barrier in
797 vitro. Frontiers in neuroscience. 2019;13:419.
798 [38] Endres K. Apolipoprotein A1, the neglected relative of Apolipoprotein E and its potential role in
799 Alzheimer's disease. Neural Regeneration Research. 2021;16.
800 [39] Fania C, Arosio B, Capitanio D, Torretta E, Gussago C, Ferri E, et al. Protein signature in
801 cerebrospinal fluid and serum of Alzheimer's disease patients: The case of apolipoprotein A-1
802 proteoforms. PLOS ONE. 2017;12:e0179280.
803 [40] Paslawski W, Zareba-Paslawska J, Zhang X, Hölzl K, Wadensten H, Shariatgorji M, et al. α-
804 synuclein–lipoprotein interactions and elevated ApoE level in cerebrospinal fluid from Parkinson's
805 disease patients. Proceedings of the National Academy of Sciences. 2019;116:15226-35.
806 [41] Paula-Lima AC, Tricerri MA, Brito-Moreira J, Bomfim TR, Oliveira FF, Magdesian MH, et al. Human
807 apolipoprotein A–I binds amyloid-β and prevents Aβ-induced neurotoxicity. The International Journal of
808 Biochemistry & Cell Biology. 2009;41:1361-70.
809 [42] Qiang JK, Wong YC, Siderowf A, Hurtig HI, Xie SX, Lee VM-Y, et al. Plasma apolipoprotein A1 as a
810 biomarker for Parkinson disease. Annals of Neurology. 2013;74:119-27.
811 [43] Song F, Poljak A, Crawford J, Kochan NA, Wen W, Cameron B, et al. Plasma Apolipoprotein Levels
812 Are Associated with Cognitive Status and Decline in a Community Cohort of Older Individuals. PLOS ONE.
813 2012;7:e34078.
814 [44] Swanson CR, Berlyand Y, Xie SX, Alcalay RN, Chahine LM, Chen-Plotkin AS. Plasma apolipoprotein A1
815 associates with age at onset and motor severity in early Parkinson's disease patients. Movement
816 Disorders. 2015;30:1648-56.
817 [45] van der Vorst EPC. High-Density Lipoproteins and Apolipoprotein A1. In: Hoeger U, Harris JR,
818 editors. Vertebrate and Invertebrate Respiratory Proteins, Lipoproteins and other Body Fluid Proteins.
819 Cham: Springer International Publishing; 2020. p. 399-420.

820 [46] Zhou Q, Zhao F, Lv Z-p, Zheng C-g, Zheng W-d, Sun L, et al. Association between APOC1
821 Polymorphism and Alzheimer's Disease: A Case-Control Study and Meta-Analysis. PLOS ONE.
822 2014;9:e87017.
823 [47] Castellano JM, Kim J, Stewart FR, Jiang H, DeMattos RB, Patterson BW, et al. Human apoE Isoforms
824 Differentially Regulate Brain Amyloid-β Peptide Clearance. Science Translational Medicine.
825 2011;3:89ra57-89ra57.
826 [48] Deane R, Sagare A, Hamm K, Parisi M, Lane S, Finn MB, et al. apoE isoform-specific disruption of
827 amyloid beta peptide clearance from mouse brain. The Journal of clinical investigation. 2008;118:4002-
828 13.
829 [49] Merino-Zamorano C, Fernández-de Retana S, Montañola A, Batlle A, Saint-Pol J, Mysiorek C, et al.
830 Modulation of Amyloid-β 1–40 Transport by ApoA1 and ApoJ Across an in vitro Model of the Blood-Brain
831 Barrier. Journal of Alzheimer's Disease. 2016;53:677-91.
832 [50] Verghese PB, Castellano JM, Garai K, Wang Y, Jiang H, Shah A, et al. ApoE influences amyloid-β (Aβ)
833 clearance despite minimal apoE/Aβ association in physiological conditions. Proceedings of the National
834 Academy of Sciences. 2013;110:E1807-E16.
835 [51] Rye K-A, Clay MA, Barter PJ. Remodelling of high density lipoproteins by plasma factors.
836 Atherosclerosis. 1999;145:227-38.
837 [52] Zhang X, Yin X, Yu H, Liu X, Yang F, Yao J, et al. Quantitative proteomic analysis of serum proteins in
838 patients with Parkinson's disease using an isobaric tag for relative and absolute quantification labeling,
839 two-dimensional liquid chromatography, and tandem mass spectrometry. Analyst. 2012;137:490-5.
840 [53] de Haan W, Out R, Berbée JFP, van der Hoogt CC, Dijk KWv, van Berkel TJC, et al. Apolipoprotein CI
841 inhibits scavenger receptor BI and increases plasma HDL levels in vivo. Biochemical and Biophysical
842 Research Communications. 2008;377:1294-8.
843 [54] Berbée JFP, Vanmierlo T, Abildayeva K, Blokland A, Jansen PJ, Lütjohann D, et al. Apolipoprotein CI
844 Knock-Out Mice Display Impaired Memory Functions. Journal of Alzheimer's Disease. 2011;23:737-47.
845 [55] Albert AD, Brad R. Parkinson disease and cognitive impairment. Neurology: Clinical Practice.
846 2016;6:452.
847 [56] Fuior EV, Gafencu AV. Apolipoprotein C1: Its Pleiotropic Effects in Lipid Metabolism and Beyond.
848 International Journal of Molecular Sciences. 2019;20:5939.

849 [57] Cudaback E, Li X, Yang Y, Yoo T, Montine KS, Craft S, et al. Apolipoprotein C-I is an APOE genotype-
850 dependent suppressor of glial activation. Journal of Neuroinflammation. 2012;9:192.
851 [58] Abildayeva K, Berbée JFP, Blokland A, Jansen PJ, Hoek FJ, Meijer O, et al. Human apolipoprotein C-I
852 expression in mice impairs learning and memory functions. Journal of Lipid Research. 2008;49:856-69.
853 [59] Association GAotWM. World Medical Association Declaration of Helsinki: ethical principles for
854 medical research involving human subjects. The Journal of the American College of Dentists. 2014;81:14.
855 [60] Deutsch EW, Bandeira N, Perez-Riverol Y, Sharma V, Carver Jeremy J, Mendoza L, et al. The
856 ProteomeXchange consortium at 10 years: 2023 update. Nucleic Acids Research. 2022;51:D1539-D48.
857 [61] Perez-Riverol Y, Bai J, Bandla C, García-Seisdedos D, Hewapathirana S, Kamatchinathan S, et al. The
858 PRIDE database resources in 2022: a hub for mass spectrometry-based proteomics evidences. Nucleic
859 Acids Research. 2021;50:D543-D52.

860

861 ## Figure Legends

862 **Figure 1** – Pipeline of sample preparation, data acquisition and data analysis.

863 **Figure 2 – Comparative differential proteomic analysis of whole and HMW serum of AD and PD**
864 **patients. (a)** Venn diagram comparing the number of quantified proteins in each sample type using
865 sample-specific libraries (solid lines; Additional File 2: Supplementary Tables 1-2). In addition,
866 quantification in whole serum was also performed for the proteins identified in the HMW-specific library
867 (dashed line; Serum&HMWLib condition; Additional File 2: Supplementary Table 3) to evaluate the
868 possible use of HMW fractionation as a tool to improve the proteome coverage of serum samples. A
869 total of 224 proteins were quantified in the serum samples using the three strategies referred above;
870 from those, 162 proteins were commonly quantified independently of the strategy, corresponding to
871 nearly three-quarters of all the quantified proteins (72.3%). Only three new proteins were quantified in
872 whole serum using the HMW-specific library. **(b)** Venn diagram comparing the total number of proteins
873 considered altered among the three experimental groups using the two different serum-processing
874 strategies used in this work (Additional File 1: Supplementary Figure 2 and Additional File 2:
875 Supplementary Tables 1-2). A total of 69 proteins were considered altered among the three
876 experimental groups; of those, only 11 proteins (the respective gene names are indicated) were
877 consistently considered altered independently of the strategy used. **(c)** Comparison of the levels of the
878 11 proteins commonly considered altered in both whole serum and HMW-fractionated serum. The
879 proteins were arranged considering the group comparison where the statistical differences were
880 observed (Additional File 1: Supplementary Figure 3), and the alterations were presented as the median
881 fold change observed in each sample type. Proteins considered altered in more than one group are
882 indicated in italic and with a grey shadow. Only one protein, the beta-2-glycoprotein 1 (indicated in
883 bold), presented a divergent tendency when considering its values in the whole serum versus after the
884 HMW fractionation of the samples. # - non-statistically significant difference.

885 **Figure 3 – Characterization of the proteins exclusively altered in whole serum or HMW serum. (a)**
886 GeneMania Network of the 28 proteins altered only at the HMW serum sample (listed in larger circles).
887 The analysis was performed with network weighting equal by network, allowing a maximum of 28 extra

888 resultant genes (non-listed small circles). The seven most enriched GeneMania Functions were
889 highlighted in the network (color code; complete results in Additional File 2: Supplementary Table 4).
890 Only protein-protein physical interactions (red edges) were considered in this analysis, demonstrating
891 that most of these 28 altered proteins have known interactors and can be involved in the formation of
892 large protein-protein complexes. **(b)** FunRich Biological Pathways enriched in the whole serum (30
893 proteins; Additional File 2: Supplementary Table 5) and HMW serum (28 proteins; Additional File 2:
894 Supplementary Table 6) proteomes. All GO analyses considered a $p < 0.05$. Pathways uniquely enriched
895 at the HMW serum or particularly enriched in this type of sample when compared to the whole serum
896 are indicated in bold.

897 **Figure 4 – Identification of potential circulating biomarkers of AD and PD. (a-c)** Venn diagrams
898 representing the distribution of the altered proteins among the different comparisons (AD vs. CT; PD vs.
899 CT; AD vs. PD) considering the whole serum, HMW serum and the combination of the two (Whole +
900 HMW serum) types of samples, respectively. **(d-f)** LDA using all altered proteins per sample type or the
901 combination of the two. The number of proteins used in each model is indicated above the graphic, and
902 for each model it is indicated their specificity (percentage of healthy individuals correctly identified;
903 indicated in black) and the sensitivity per disease condition (percentage of AD or PD patients correctly
904 identified; indicated in red and blue, respectively). Specificity and sensitivity values were also
905 summarized in Additional File 2: Supplementary Table 7, and the generated LDA discriminant functions
906 and their respective statistical confidence were summarized in Table 2. **(g-h)** Comparative ROC curves of
907 the discriminant functions generated using all altered proteins per sample type or a combination of the
908 two. An independent evaluation was performed for each disease group being studied. The AUC of the
909 ROC curves, their 95% CI and the pairwise comparisons are summarized in **(i)**. CI was calculated as
910 follows AUC ± 1.96 SE. n.s., non-significant alterations. * and # indicate a $p < 0.05$ for statistically
911 significant differences in comparison to the Whole Serum or HMW+Whole Serum in comparison to
912 HMW Serum, respectively, using the method of Delong et al. (1988) [22].

913 **Figure 5 – Characterization of the protein panel selected by the combined LDA model. (a)** Violin plots
914 representing the protein level distribution of the ten proteins from the model. The dashed lines indicate
915 the first, second (median) and third quartiles. *, **, and *** indicate a $p < 0.05$, $p<0.01$, and $p<0.001$

916 for statistically significant differences. * denotes the comparison to control and # the differences
917 between disease groups. Statistical analysis was performed using the Kruskal–Wallis H test followed by
918 the Dunn's Test for pairwise comparison. **(b)** Pearson's correlation analysis between the overall
919 regulation profile of the proteins included in the model. **(c)** Heatmap and hierarchical clustering analysis
920 of the proteins from the model. Clustering was performed for both proteins and individuals. Three
921 different clusters (Cluster PD, CT and AD) containing the large majority of the individuals from a given
922 group can be highlighted from the analysis. The average profile of each cluster is indicated on the right
923 and can be considered as the profile of expression of those proteins within the groups considered in this
924 study. **(d)** Interaction network of these proteins carried out with STRING with a medium confidence (0.4)
925 score. The color of the edges indicates the type of evidence that supports the interaction, while the
926 color of the nodes represents the categorization of the proteins considering UniProt Keywords. The
927 calculated PPI enrichment p-value is 2.07e-05. Three clusters (Cluster 1 to 3) can be identified within the
928 network, with the dashed edges indicating the separation between clusters. Cluster 1 corresponds to
929 proteins whose interactions are experimentally confirmed, cluster 2 is composed of theoretically related
930 proteins, and cluster 3 corresponds to non-related proteins. **(e)** Reactome pathways enrichment analysis
931 using the proteins from the model. The red line indicates Bonferroni's corrected p-value with the
932 corrected $p < 0.05$, meaning a significant enrichment. The grey dashed line indicates the reference line
933 ($p = 0.05$).

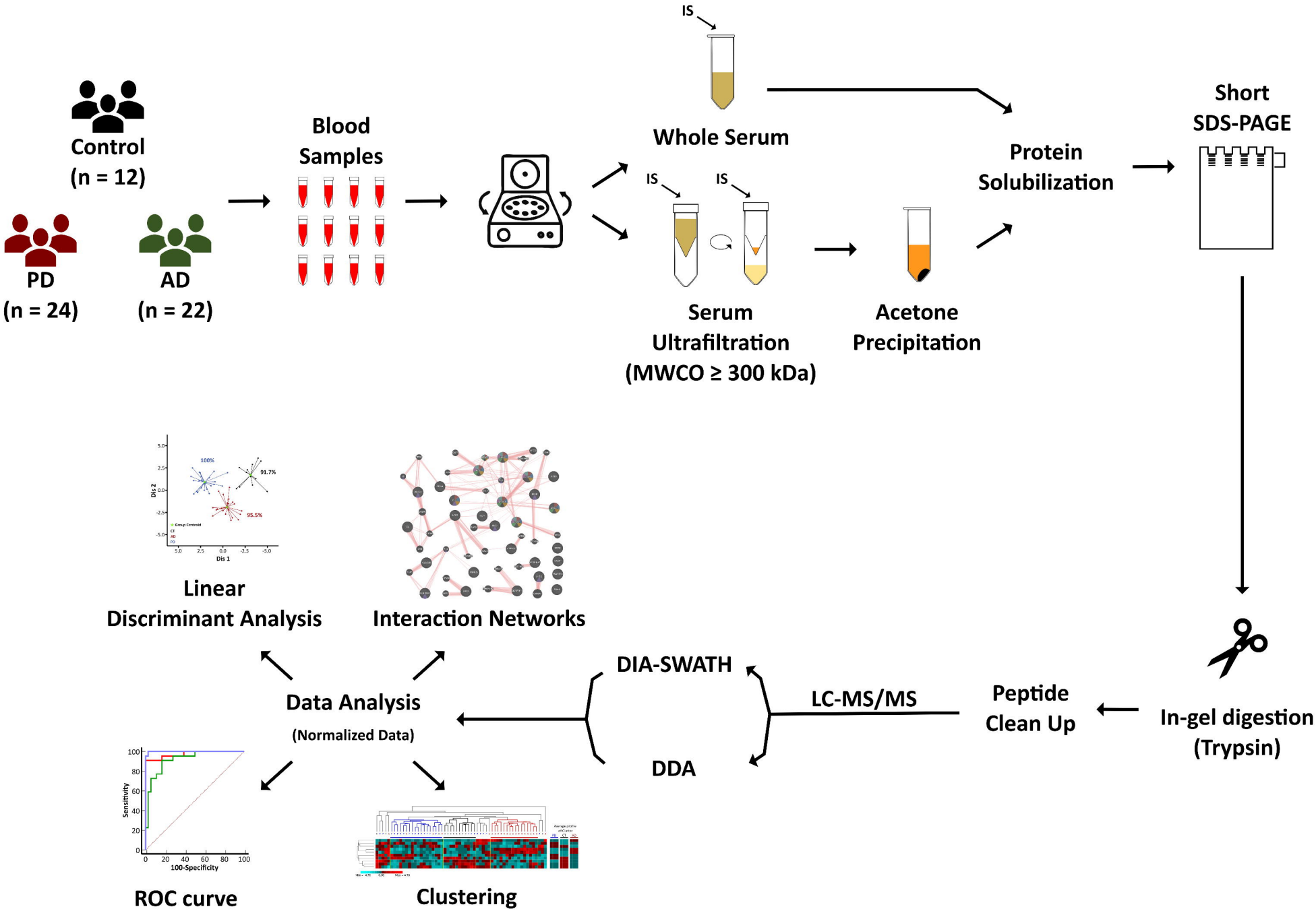
Control
(n = 12)
PD
(n = 24)
AD
(n = 22)
Blood
Samples
IS
Whole Serum
IS
IS
Serum
Ultrafiltration
(MWCO ≥ 300 kDa)
Acetone
Precipitation
Protein
Solubilization
Short
SDS-PAGE
In-gel digestion
(Trypsin)
Peptide
Clean Up
LC-MS/MS
DIA-SWATH
DDA
Data Analysis
(Normalized Data)
Linear
Discriminant Analysis
Interaction Networks
ROC curve
Clustering

(a)

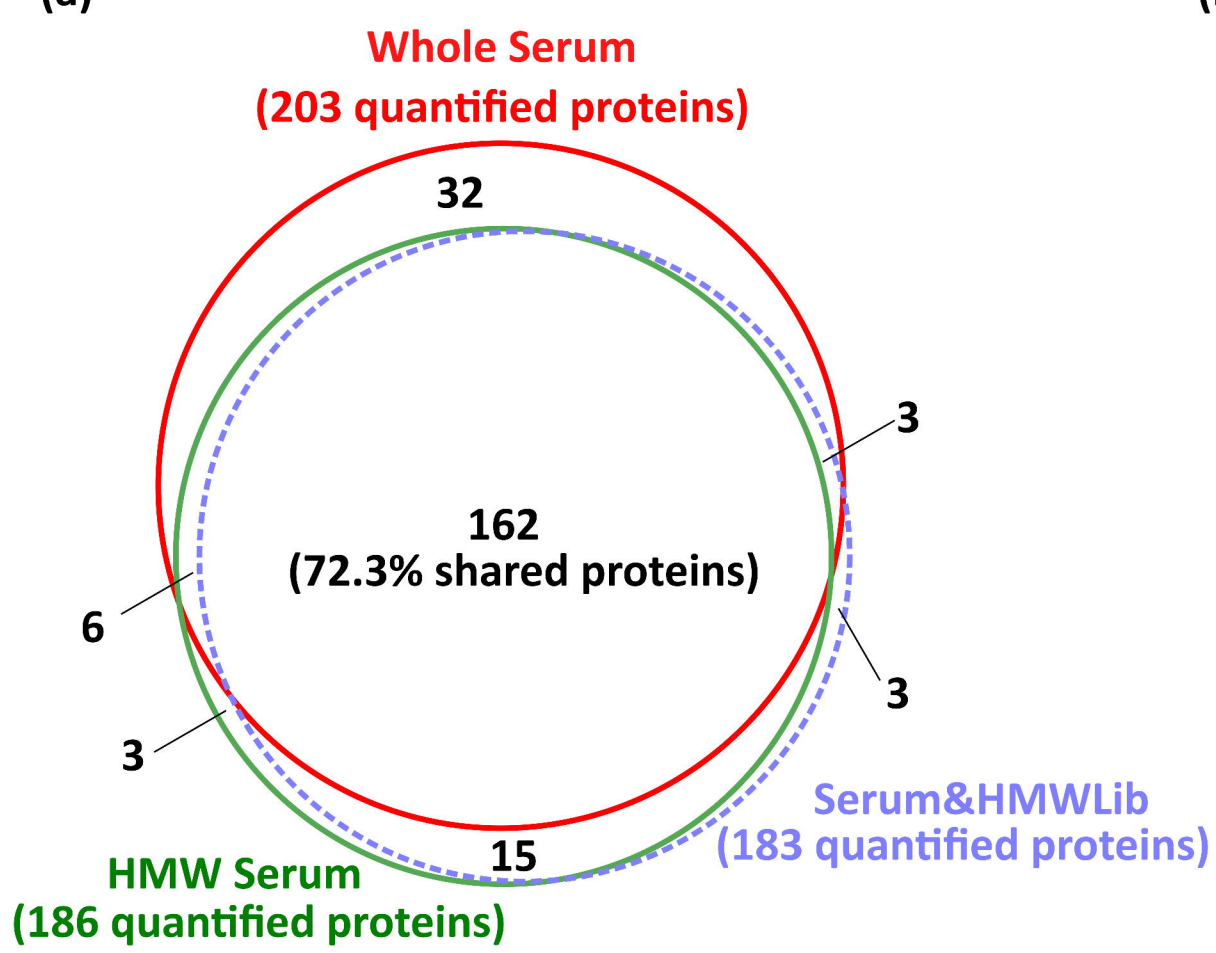

Total: 224 quantified proteins

(b)

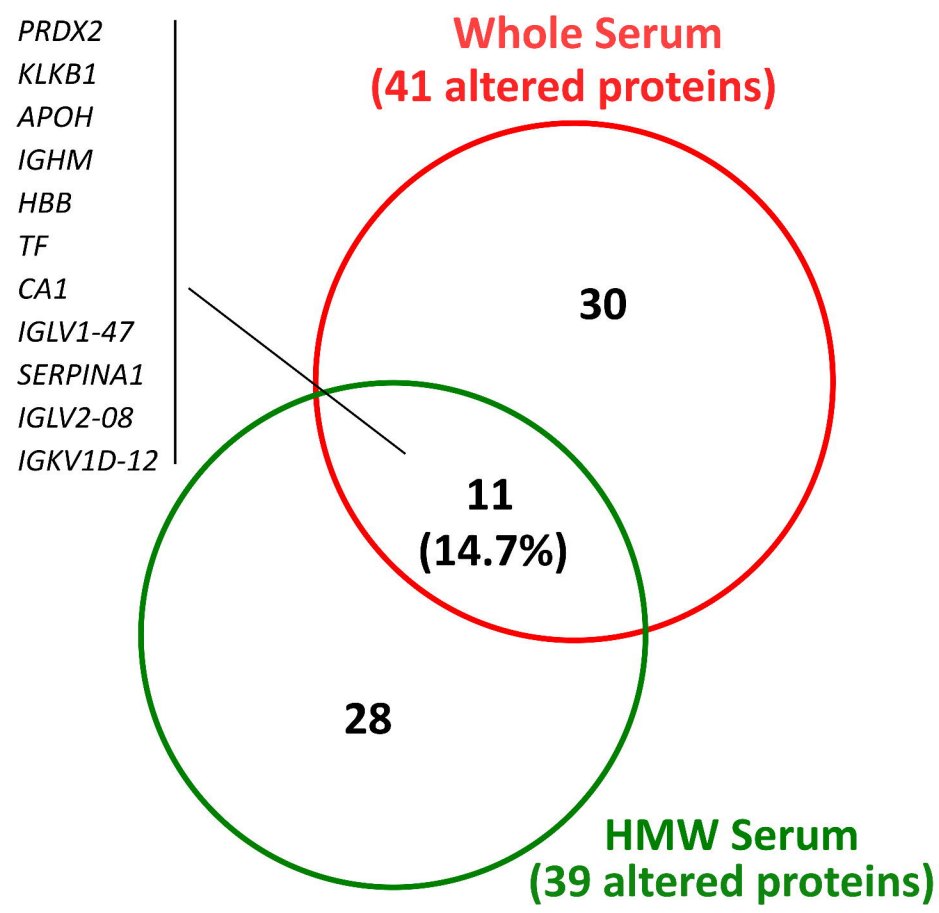

Total: 69 altered proteins

(c)

Group comparison	Gene Name	Protein Name	Fold Change Serum	Fold Change HMW
AD vs CT	*APOH*	Beta-2-glycoprotein 1 (APC inhibitor)	1.008#	0.676
	CA1	Carbonic anhydrase 1	2.467	2.397
	IGKV1D-12	Immunoglobulin kappa variable 1D-12	0.799	0.762
	IGLV1-47	*Immunoglobulin lambda variable 1-47*	0.767	0.786
	IGHM	Immunoglobulin heavy constant mu	0.372	0.692
	TF	Serotransferrin	0.856	0.792
	KLKB1	Plasma kallikrein	0.807	0.707
	PRDX2	*Peroxiredoxin-2*	2.691	2.979
	HBB	*Hemoglobin subunit beta*	3.958	3.129
PD vs CT	*SERPINA1*	Alpha-1-antitrypsin	0.877	0.752
AD vs PD	*APOH*	Beta-2-glycoprotein 1 (APC inhibitor)	1.238	0.803#
	CA1	Carbonic anhydrase 1	1.977	1.943
	IGLV1-47	*Immunoglobulin lambda variable 1-47*	0.894	0.785
	IGLV2-8	Immunoglobulin lambda variable 2-8	0.777	0.788
	PRDX2	*Peroxiredoxin-2*	1.749	2.568
	HBB	*Hemoglobin subunit beta*	2.622	2.094

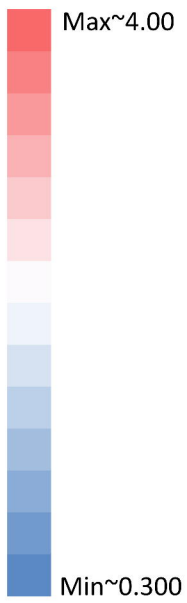

(a)

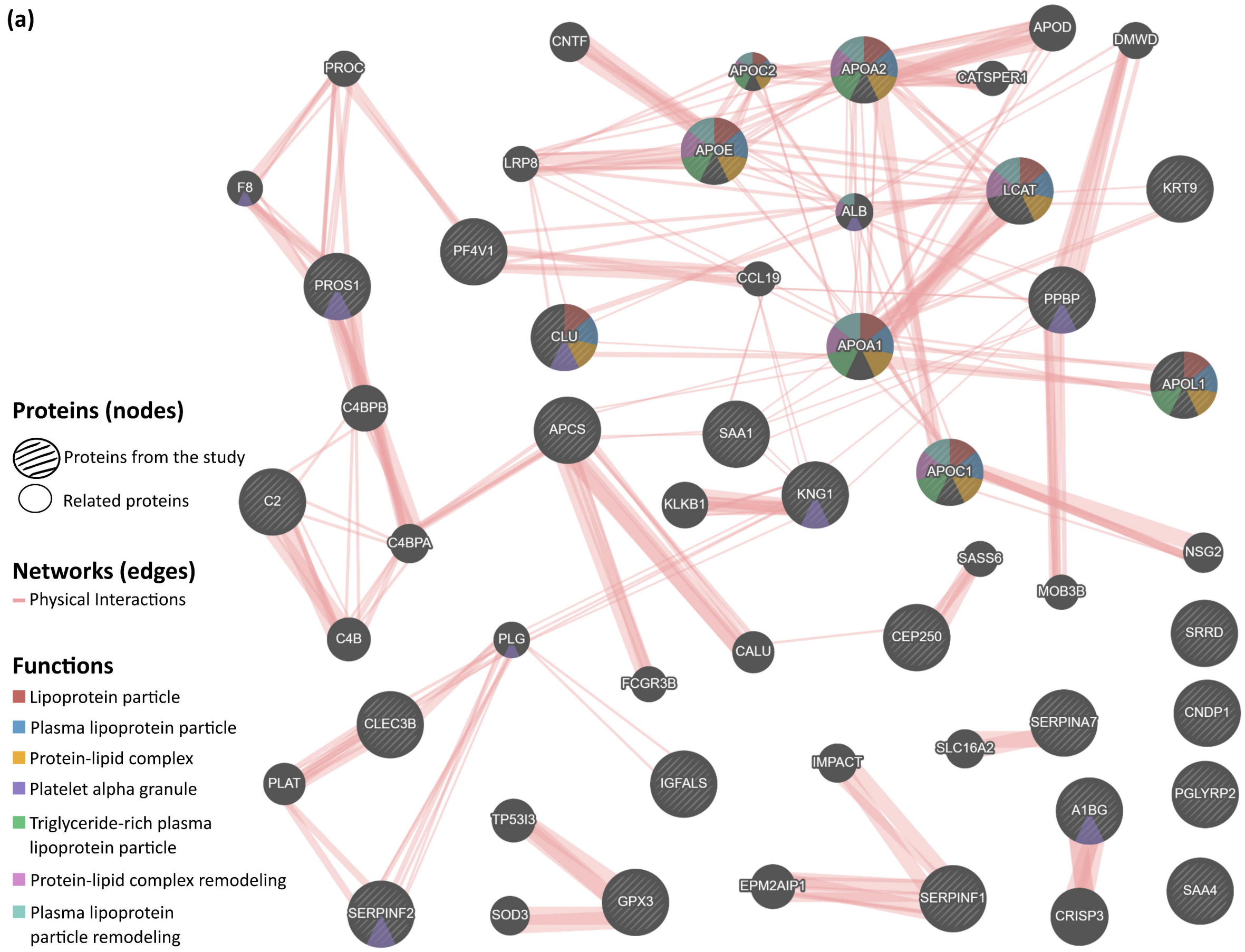
Proteins (nodes)
Proteins from the study
Related proteins
Networks (edges)
Physical Interactions
Functions
Lipoprotein particle
Plasma lipoprotein particle
Protein-lipid complex
Platelet alpha granule
Triglyceride-rich plasma lipoprotein particle
Protein-lipid complex remodeling
Plasma lipoprotein particle remodeling
CNTF
APOD
DMWD
PROC
APOC2
APOA2
CATSPER1
APOE
LRP8
F8
LCAT
KRT9
ALB
PF4V1
PROS1
CCL19
PPBP
CLU
APOA1
APOL1
C4BPB
APCS
SAA1
APOC1
C2
KLKB1
KNG1
C4BPA
NSG2
SASS6
MOB3B
C4B
PLG
CALU
CEP250
SRRD
FCGR3B
CLEC3B
SERPINA7
CNDP1
SLC16A2
IMPACT
PLAT
IGFALS
A1BG
PGLYRP2
TP53I3
EPM2AIP1
SERPINF1
SAA4
GPX3
SERPINF2
SOD3
CRISP3

(b)

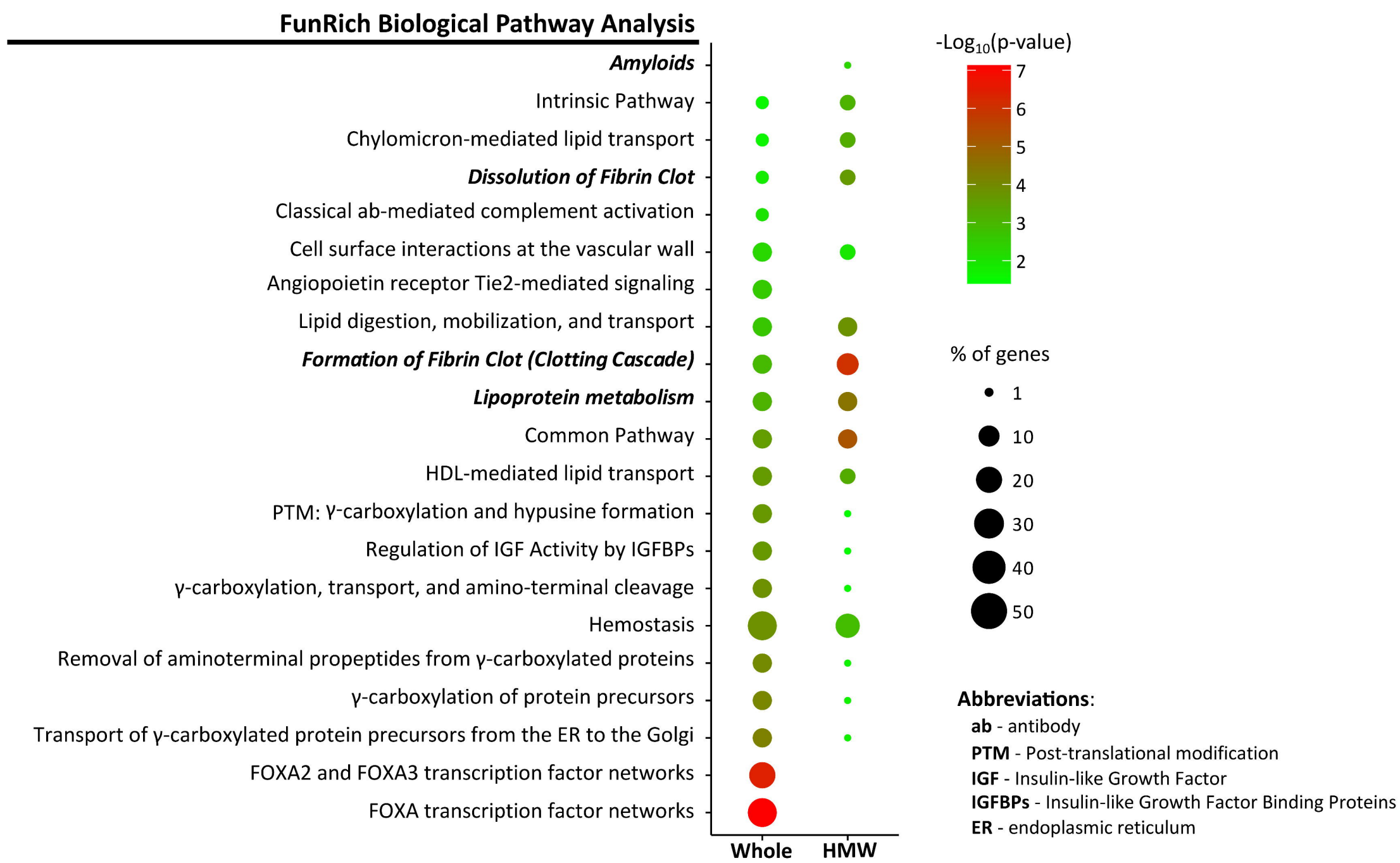
FunRich Biological Pathway Analysis
Amyloids
Intrinsic Pathway
Chylomicron-mediated lipid transport
Dissolution of Fibrin Clot
Classical ab-mediated complement activation
Cell surface interactions at the vascular wall
Angiopoietin receptor Tie2-mediated signaling
Lipid digestion, mobilization, and transport
Formation of Fibrin Clot (Clotting Cascade)
Lipoprotein metabolism
Common Pathway
HDL-mediated lipid transport
PTM: γ-carboxylation and hypusine formation
Regulation of IGF Activity by IGFBPs
γ-carboxylation, transport, and amino-terminal cleavage
Hemostasis
Removal of aminoterminal propeptides from γ-carboxylated proteins
γ-carboxylation of protein precursors
Transport of γ-carboxylated protein precursors from the ER to the Golgi
FOXA2 and FOXA3 transcription factor networks
FOXA transcription factor networks
Whole
HMW
-Log10(p-value)
7
6
5
4
3
2
% of genes
1
10
20
30
40
50
Abbreviations:
ab - antibody
PTM - Post-translational modification
IGF - Insulin-like Growth Factor
IGFBPs - Insulin-like Growth Factor Binding Proteins
ER - endoplasmic reticulum

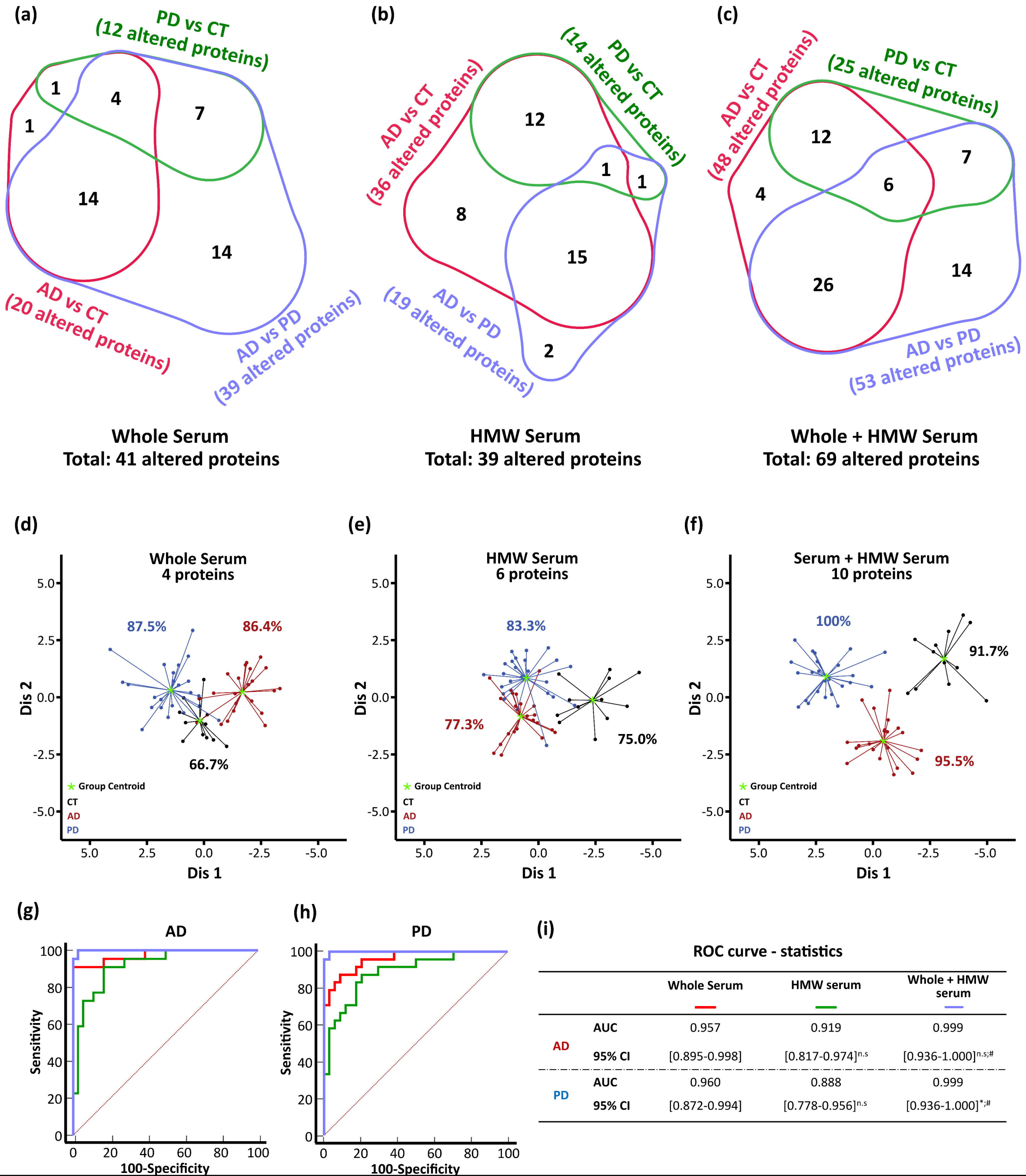

(i)

ROC curve - statistics

		Whole Serum	HMW serum	Whole + HMW serum
AD	AUC	0.957	0.919	0.999
	95% CI	[0.895-0.998]	[0.817-0.974]$^{n.s}$	[0.936-1.000]$^{n.s;\#}$
PD	AUC	0.960	0.888	0.999
	95% CI	[0.872-0.994]	[0.778-0.956]$^{n.s}$	[0.936-1.000]$^{*;\#}$

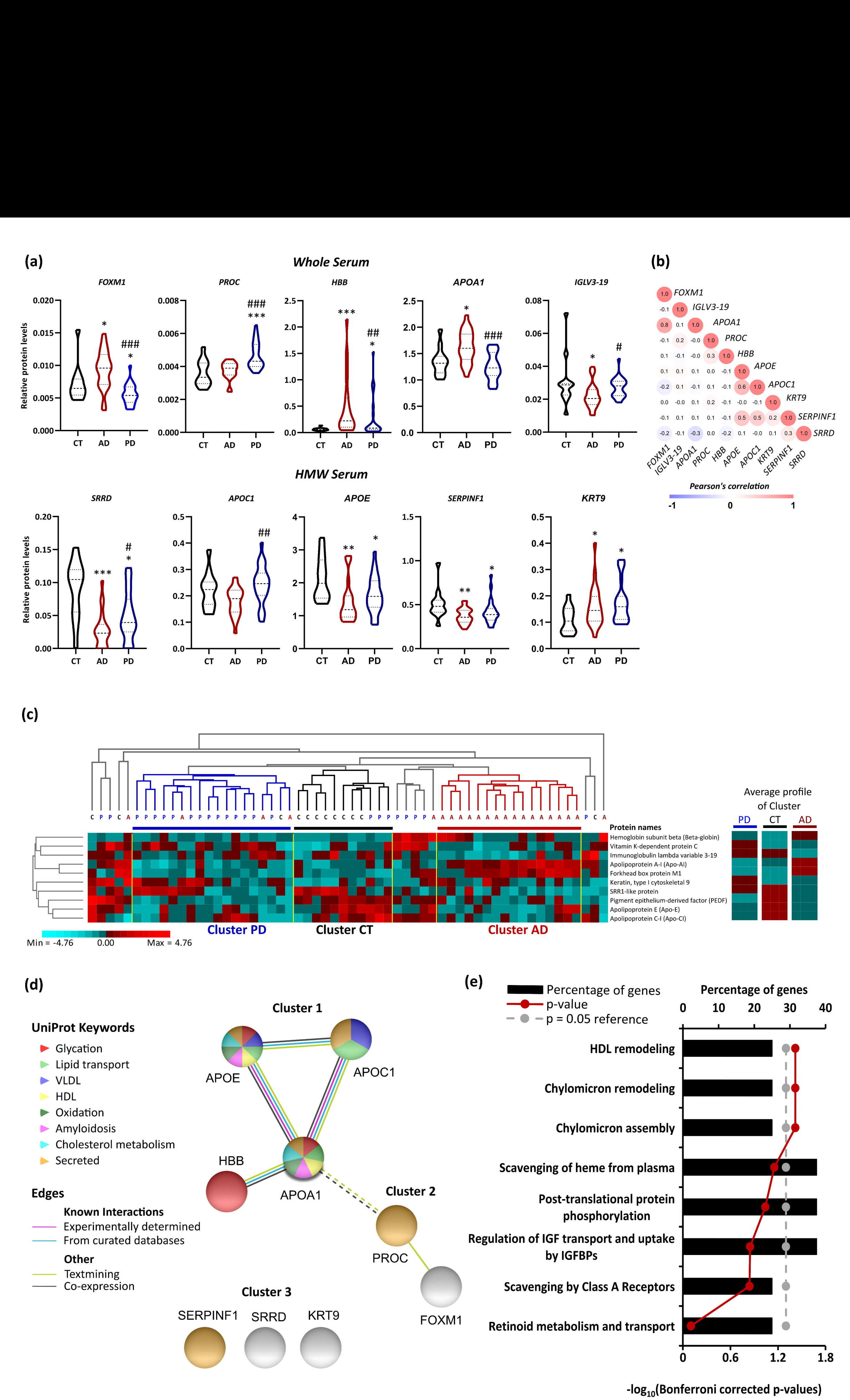
(a)
Whole Serum
FOXM1
PROC
HBB
APOA1
IGLV3-19
Relative protein levels
CT
AD
PD
HMW Serum
SRRD
APOC1
APOE
SERPINF1
KRT9
(b)
FOXM1
IGLV3-19
APOA1
PROC
HBB
APOE
APOC1
KRT9
SERPINF1
SRRD
Pearson's correlation
-1
0
1
(c)
Protein names
Hemoglobin subunit beta (Beta-globin)
Vitamin K-dependent protein C
Immunoglobulin lambda variable 3-19
Apolipoprotein A-I (Apo-AI)
Forkhead box protein M1
Keratin, type I cytoskeletal 9
SRR1-like protein
Pigment epithelium-derived factor (PEDF)
Apolipoprotein E (Apo-E)
Apolipoprotein C-I (Apo-CI)
Average profile of Cluster
PD
CT
AD
Cluster PD
Cluster CT
Cluster AD
Min = -4.76
0.00
Max = 4.76
(d)
UniProt Keywords
Glycation
Lipid transport
VLDL
HDL
Oxidation
Amyloidosis
Cholesterol metabolism
Secreted
Edges
Known Interactions
Experimentally determined
From curated databases
Other
Textmining
Co-expression
Cluster 1
APOE
APOC1
HBB
APOA1
Cluster 2
PROC
FOXM1
Cluster 3
SERPINF1
SRRD
KRT9
(e)
Percentage of genes
p-value
p = 0.05 reference
Percentage of genes
HDL remodeling
Chylomicron remodeling
Chylomicron assembly
Scavenging of heme from plasma
Post-translational protein phosphorylation
Regulation of IGF transport and uptake by IGFBPs
Scavenging by Class A Receptors
Retinoid metabolism and transport
-log10(Bonferroni corrected p-values)